2018

The zinc finger transcription factor PLAGL2 enhances stem cell fate and activates expression of ASCL2 in intestinal epithelial cells

Ashlee M. Strubberg
Washington University School of Medicine in St. Louis

Daniel A. Veronese Paniagua
Washington University School of Medicine in St. Louis

Tingting Zhao
First Hospital of China Medical University

Leeran Dublin
Washington University School of Medicine in St. Louis

Thomas Pritchard
Washington University School of Medicine in St. Louis

See next page for additional authors

Stem Cell Reports
Article

OPEN ACCESS

The Zinc Finger Transcription Factor PLAGL2 Enhances Stem Cell Fate and Activates Expression of *ASCL2* in Intestinal Epithelial Cells

Ashlee M. Strubberg,[1] Daniel A. Veronese Paniagua,[1] Tingting Zhao,[3] Leeran Dublin,[2] Thomas Pritchard,[1] Peter O. Bayguinov,[4] James A.J. Fitzpatrick,[4,5,6] and Blair B. Madison[1,*]

[1]Department of Medicine, Division of Gastroenterology, Washington University School of Medicine, 660 S. Euclid Avenue, Campus Box 8124, CSRB NT 923, Saint Louis, MO 63110, USA
[2]Washington University School of Medicine, Saint Louis, MO 63110, USA
[3]Department of Breast Surgery, First Hospital of China Medical University, Shenyang 110001, China
[4]Washington University Center for Cellular Imaging, Washington University School of Medicine, Saint Louis, MO 63110, USA
[5]Departments of Cell Biology & Physiology and Neuroscience, Washington University School of Medicine, Saint Louis, MO 63110, USA
[6]Department of Biomedical Engineering, Washington University in St. Louis, Saint Louis, MO 63105, USA
*Correspondence: bmadison@wustl.edu
https://doi.org/10.1016/j.stemcr.2018.06.009

SUMMARY

Intestinal epithelial stem cell (IESC) fate is promoted by two major transcriptional regulators, the TCF4/β-catenin complex and ASCL2, which drive expression of IESC-specific factors, including *Lgr5*, *Ephb2*, and *Rnf43*. Canonical Wnt signaling via TCF4/β-catenin directly transactivates *Ascl2*, which in turn auto-regulates its own expression. Conversely, Let-7 microRNAs antagonize the IESC lineage by repressing specific mRNA targets. Here, we identify the zinc finger transcription factor PLAGL2 as a Let-7 target that regulates IESC fate. PLAGL2 drives an IESC expression signature, activates Wnt gene expression, and enhances a TCF/LEF reporter in intestinal organoids. In parallel, via cell-autonomous mechanisms, PLAGL2 is required for lineage clonal expansion and directly enhances expression of *ASCL2*. PLAGL2 also supports enteroid growth and survival in the context of Wnt ligand depletion. PLAGL2 expression is strongly associated with an IESC signature in colorectal cancer and may be responsible for contributing to the aberrant activation of an immature phenotype.

INTRODUCTION

Intestinal epithelial stem cells (IESCs) reside in intestinal crypts and give rise to all endodermally derived lineages of the epithelium. The IESC consists of at least two distinct populations. The first is actively dividing, expresses high levels of the GPCR class A receptor LGR5 (Barker et al., 2007), is located at the base of intestinal crypts (Barker et al., 2007), and is highly dependent on Wnt signaling (de Lau et al., 2011; Yan et al., 2017). A second quiescent IESC is located near the base of crypts (Li et al., 2014; Sangiorgi and Capecchi, 2008; Takeda et al., 2011; Tian et al., 2011; Yan et al., 2012) and has properties of a secretory progenitor (Buczacki et al., 2013). Wnt signaling is necessary for the establishment of IESCs in post-natal intestinal development in mice (Korinek et al., 1998; Pinto et al., 2003). *Ascl2* is also required for IESC specification (van der Flier et al., 2009), and maintenance of IESCs, through cooperation with TCF4 and β-catenin to transactivate genes such as *Lgr5* and *Sox9* (Schuijers et al., 2015).

Let-7 microRNAs (miRNAs) are key regulators of cellular proliferation and differentiation in a variety of contexts and organisms, from *C. elegans* (Lee and Ambros, 2001; Slack et al., 2000) to humans. Let-7 frequently acts to repress stem cell fate or proliferation, as observed in fetal hematopoietic stem cells (Copley et al., 2013; Oshima et al., 2016; Rowe et al., 2016), neural stem cells (Rybak et al., 2008; Zhao et al., 2010), primordial germ cells (Tran et al., 2016; West et al., 2009), and IECs (Madison et al., 2015). The RNA-binding proteins, LIN28A and LIN28B, directly inhibit Let-7 in stem and progenitor cells (Hagan et al., 2009; Rahkonen et al., 2016). LIN28 proteins block Let-7 miRNA function by preventing Let-7 post-transcriptional maturation (Hagan et al., 2009; Heo et al., 2008; Piskounova et al., 2008; Viswanathan et al., 2008). Depletion of Let-7 miRNAs is frequently observed in cancer, and directly contributes to epithelial transformation in colorectal cancer (CRC) (King et al., 2011), while depletion in the mouse intestine via transgenic LIN28A/B expression drives the formation of spontaneous, aggressive adenocarcinomas (Madison et al., 2013; Tu et al., 2015). LIN28 proteins are expressed in the developing mouse gut, but only LIN28B is detectable in the adult intestine, exhibiting nuclear localization in the epithelial crypt compartment (Madison et al., 2013). In mouse models, overexpression of LIN28B in the intestinal epithelium augments the expression of stem cell markers and enhances colony-forming potential of small intestinal organoids (enteroids) (Madison et al., 2013, 2015). Consistent with this, levels of Let-7a and Let-7b miRNAs are inversely proportional to mRNA levels of *LGR5* and *EPHB2* in human CRC, which represent classical IESC markers (Madison et al., 2015). Further examination of Let-7 targets that mediate these effects revealed that the canonical Let-7 target *Hmga2* is required for LIN28B-driven enhancement of colony-forming potential in mouse enteroids (Madison et al., 2015).

However, HMGA2 overexpression in mouse enteroids does not alter the abundance of any IESC marker and only drives a modest enhancement of colony-forming potential (Madison et al., 2015).

Here we identify *PLAGL2* as a Let-7 target that is strongly associated with an IESC signature. *PLAGL2* encodes a zinc finger transcription factor found within a genomic region at 20q11.21 that is frequently amplified in CRC (Carvalho et al., 2009; He et al., 2003; Hermsen et al., 2002). *PLAGL2* is expressed at high levels in various tissues of the developing fetus and placenta and plays a critical role in late intestinal epithelial differentiation (Van Dyck et al., 2007). We have reported that PLAGL2 levels are enhanced by overexpression of LIN28B in the intestinal epithelium (Madison et al., 2015), consistent with its inverse correlation with Let-7 levels in CRC (Madison et al., 2015). We find here that *PLAGL2* is a direct Let-7 target that drives stem cell fate and is required for stem cell function in organoids. One mechanism involves the direct downstream activation of the IESC lineage factor *ASCL2,* where we find that PLAGL2 binds to a conserved consensus sequence in the proximal *ASCL2* promoter.

RESULTS

Interrogation of TCGA CRC RNA sequencing (RNA-seq) datasets reveals that *PLAGL2* expression correlates highly with multiple lineage factors specific for—or highly enriched in—CBC IESCs (Munoz et al., 2012; Sato et al., 2011), including *ASCL2*, *EPHB2*, *NOTCH1*, *RNF43*, and *MYC* (Figure S1A). Among patient-derived CRC xenograft lines (Uronis et al., 2012), this trend is also evident, with significant correlation between *PLAGL2* and *ASCL2*, *RNF43*, and *NOTCH1* (Figure S1B). In a dataset of human colorectal adenomas (Sabates-Bellver et al., 2007), we also observe the co-expression of *PLAGL2* with CBC IESC markers, which are coordinately upregulated together in adenomas relative to normal tissue (Figure S1C).

We used human intestinal organoids to examine the relationship of LIN28B-Let-7, PLAGL2, and effects on stem cells. As expected, LIN28B overexpression in organoids enhances colony-forming potential (Figure 1A). *PLAGL2*, along with the validated Let-7 target, *HMGA2*, is upregulated in a pattern similar to *ASCL2* in these organoids (Figure 1B). *PLAGL2* upregulation in the intestinal epithelium, downstream of LIN28B, is also observed in our mouse models of LIN28B overexpression (Madison et al., 2015). Thus, *PLAGL2* activation is a downstream feature of LIN28B-mediated enhancement of stem cell activity.

To definitively classify *PLAGL2* as a Let-7 target, we pursued validation in *in vitro* models. Transfection of a Let-7b miRNA mimic into DLD1 CRC cells caused a significant depletion of *PLAGL2* mRNA (Figure 1C). We also developed a heterologous reporter system with destabilized GFP and RFP proteins for real-time evaluation of Let-7 miRNA repression (Figure 1D). In the context of a synthetic array of seven Let-7 target sites, reporter activity is repressed 60%–70% by Let-7a (Figure 1E). Likewise, assays of the *PLAGL2* 3′ UTR reveal a 40% decrease of reporter activity by Let-7a (Figure 1F) that is completely abrogated by mutations in each of two Let-7 recognition sequences in the *PLAGL2* 3′ UTR (Figure 1F). Thus, this supports our hypothesis that *PLAGL2* is directly repressed by Let-7.

To model the aberrant upregulation of *PLAGL2* that is likely within the context of Let-7 loss, *LIN28B* de-repression, or 20q11.21 amplification, we generated murine enteroids constitutively overexpressing hemagglutinin-tagged PLAGL2. This yielded modest expression of PLAGL2 protein in two separate clones (Figure 2A). PLAGL2 expression causes a marked increase in cyst-like enteroids (Figures 2B–2D). PLAGL2-expressing enteroids also exhibit a dose-dependent increase in colony-forming potential (Figures 2E and 2F). Similar effects were observed upon PLAGL2 expression in human colonic organoids, with an augmentation of colony-forming potential (Figure 2G). In human organoids, we observe enhancement of proliferation as measured by 5-ethynyl-2′-deoxyuridine incorporation (Figures 2H–2J). This effect is only evident when organoids are cultured in medium lacking Wnt3a. Inactivation of *Plagl2* in mouse enteroids with CRISPR/Cas revealed defects in colony-forming potential of mutants (Figures 2K–2M). However, no significant changes in enteroid growth were observed (Figure 2N). To gain insight into the cell-autonomous function of PLAGL2, we performed lineage-tracing experiments in enteroids stably expressing the $Cas9^{D10A}$ nuclease followed by stable transfection with a transposon constitutively expressing both GFP and gRNAs against *Plagl2*. Following transfection, the majority of surviving organoids do not contain GFP-positive transfected cells. However, a minority (~2%) show evidence of clonal expansion of GFP-positive clones, while targeted inactivation of *Plagl2* causes a reduction in these lineage-tracing events (Figure 2O), as observed over 7 days following the transfection (Figure 2P). Thus, PLAGL2 supports the stem cell lineage in a cell-autonomous manner in enteroids.

To gain insight into pathways operating downstream of PLAGL2 we performed RNA-seq in two mouse enteroid clones overexpressing PLAGL2 (Figure 3A). Because PLAGL2 appears to drive stem cell fate in enteroids, we performed gene set enrichment analysis (GSEA) (Subramanian et al., 2005) on PLAGL2-induced mRNAs in comparison with an expression dataset for GFP-sorted CBC IESCs from *Lgr5-EGFP* mice (Barker et al., 2007; Munoz et al., 2012). This reveals significant enrichment (Figure 3B), indicating that PLAGL2 drives a CBC stem cell expression

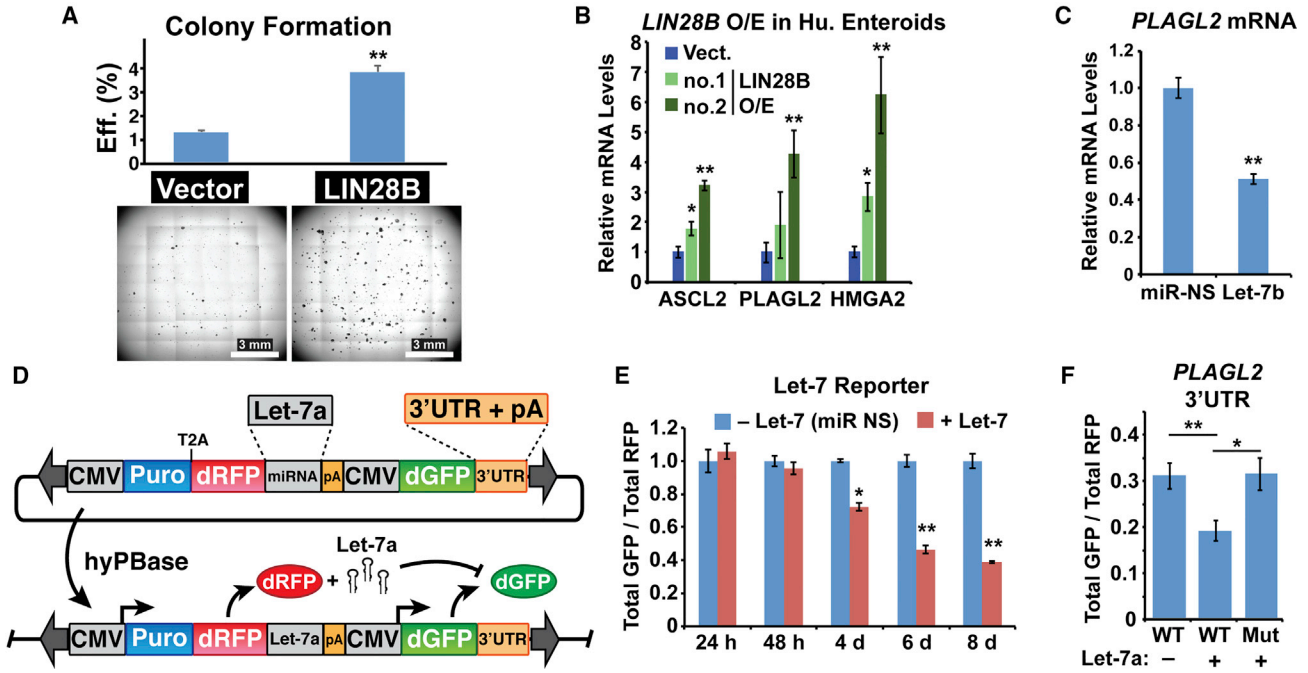

Figure 1. PLAGL2 Is Directly Repressed by Let-7 miRNAs

(A) Human organoids were plated as single cells in Matrigel for a colony-forming assay, in quadruplicate. Colonies were counted after 7 days in culture.

(B) Expression levels of *PLAGL2*, *HMGA2*, and *ASCL2* were assayed in two human organoid clones constitutively expressing LIN28B (LIN28B O/E).

(C) Transient transfection of DLD1 cells with a Let-7b miRNA mimic causes the depletion of endogenous *PLAGL2* mRNA, as assayed by RT-PCR 72 hr after transfection.

(D) Schematic of a transposon miRNA reporter vector for assaying effects of Let-7a on the *PLAGL2* 3′ UTR.

(E) Validation of the miRNA reporter vector containing a synthetic Let-7 target with seven repeats of the Let-7 target seed sequence.

(F) The miRNA reporter vector containing the *PLAGL2* 3′ UTR and a non-specific miRNA or Let-7a. Mutation (Mut) of both Let-7 target seed sequences in the *PLAGL2* 3′ UTR renders the reporter resistant to Let-7.

Student's one-tailed t test was performed to evaluate significance between means of replicates, where *$p < 0.05$ and **$p < 0.01$.

signature. This was true for both PLAGL2 clone no. 1 (false discovery rate [FDR] $q < 0.001$) and no. 2 (FDR $q < 0.02$). An unbiased GSEA query of all molecular function gene ontology gene sets reveals that PLAGL2-upregulated transcripts are enriched for genes associated with Frizzled binding (Figure 3C), both for PLAGL2 clone no. 1 (FDR $q = 0.164$) and no. 2 (FDR $q = 0.317$). Further examination reveals several Wnt ligands (*Wnt9b*, *Wnt4*, *Wnt10a*, and *Wnt5a*) are upregulated by PLAGL2 (Figure 3D), which was validated by RT-PCR (Figure 3E). Decreased expression of Wnt target genes, *Cd44* and *Axin2*, in *Plagl2* null enteroids also supported a positive role for PLAGL2 in driving canonical Wnt signaling (Figure 3F).

To gauge effects on Wnt we generated enteroids with a stable TCF/LEF reporter transgene driving expression of nuclear localized tdTomato (TOP-tdT, Figure 3G), which exhibited the expected sensitivity to manipulation of Wnt signaling with GSK3β and Porcupine inhibitors (Figures 3H and 3I). Transgenic co-expression of PLAGL2 in enteroids caused a marked increase in the number of TOP-tdT-positive cells (Figures 3J–3O), although upregulation of TOP-tdT reporter activity within each individual cell appeared variable (Figure 3P) and did not correlate with levels of overexpressed *PLAGL2* mRNA (Figure 3Q). To better measure possible effects of secreted signals on TOP-tdT reporter activity, GFP-labeled wild-type (WT) TOP-tdT enteroids were co-cultured with PLAGL2-expressing enteroids (Figure 3R). Reporter activity in GFP-labeled co-cultured enteroids was enhanced by these PLAGL2 enteroids (Figure 3S). Consistent with an enhancement of Wnt signaling, colony-forming potential was augmented in WT *ROSA26*^{mTmG} enteroids co-cultured with PLAGL2 enteroids (Figure 3T). Thus, PLAGL2 drives modest enhancement of canonical Wnt signaling, non-cell-autonomously.

To determine if Wnt signaling is the primary underlying driver of the PLAGL2 phenotype in enteroids, we treated

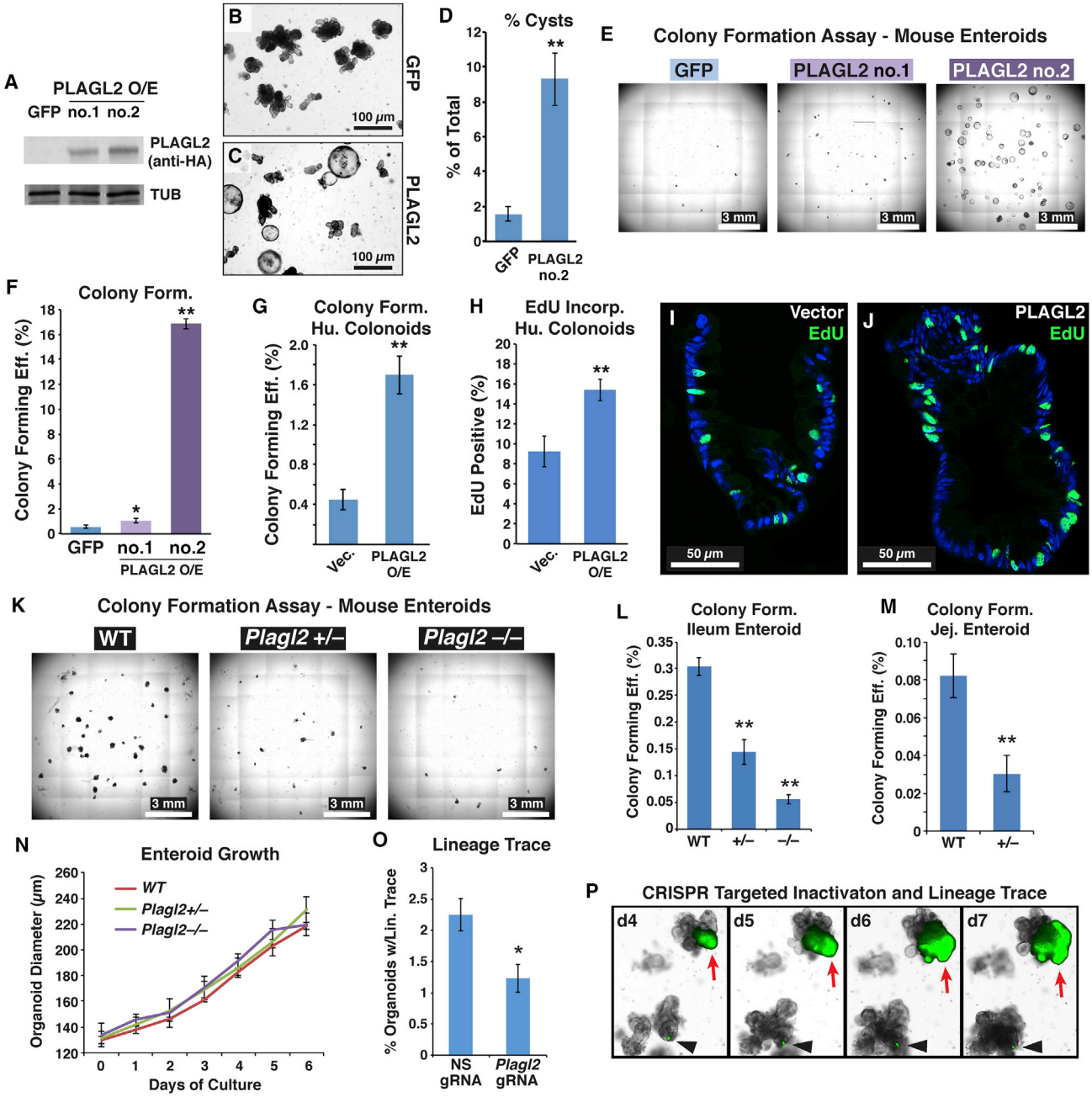

Figure 2. PLAGL2 Drives Stem Cell Potential in Enteroids

(A) Mouse enteroids stably overexpressing (O/E) hemagglutinin-tagged *PLAGL2* or GFP were evaluated by immunoblot.

(B–D) GFP-expressing enteroids appeared morphologically similar to un-transfected parental enteroids (not shown) (B), whereas *PLAGL2* O/E enteroids (clone no. 2) frequently formed large cysts (C), quantified in (D).

(E and F) Stitched representative microscopic images of colony-forming assay (CFA) of *PLAGL2* O/E mouse enteroids, performed in quadruplicate (E), which are quantified in (F).

(G) Quantification of colony-forming assay of *PLAGL2*-expressing human colonoids.

(H–J) 5-Ethynyl-2′-deoxyuridine (EdU) incorporation in human colonoids as quantified in sections (H), with representative images for empty vector (I) and *PLAGL2*-expressing human colonoids (J).

(K–M) Representative images of CFA of *Plagl2* mutant mouse ileum enteroids, performed in quadruplicate (K), which are quantified in (L), while *Plagl2* mutant mouse jejunum enteroids are quantified in (M).

(N) *Plagl2* mutant mouse enteroid size over 6 days of culture.

(legend continued on next page)

cultures with IWP-2, a small molecule that blocks Wnt palmitoylation and secretion through inhibition of Porcupine (Chen et al., 2009). After 5–7 days of IWP-2 treatment the vast majority of control (GFP-expressing) enteroids die, while surviving enteroids eventually regress (Figure 4A). However, many PLAGL2-expressing enteroids survive IWP-2 treatment, either as cysts or budding structures (Figure 4B), which is never observed in controls (Figure 4C). To further parse Wnt dependency, PLAGL2 enteroids with the TOP-tdT reporter were treated with IWP-2 and closely monitored for reporter activity (Figures 4D–4F). Despite Wnt inhibition, PLAGL2 enteroids maintain higher expression levels of the IESC lineage markers *Ascl2* and *Lgr5* (Figure 4G), but do not drive higher expression of other Wnt target genes (Figure 4H). To see if PLAGL2 maintains stem cell potential in the face of Wnt inhibition, we continued IWP-2 treatment of enteroids (from Figures 4E and 4F) for 2 additional days, confirmed complete loss of the TOP-tdT reporter in each enteroid, and then re-plated remaining enteroids in fresh medium lacking IWP-2. PLAGL2-expressing enteroids yielded significantly more numerous new colonies, relative to the initial number of enteroids (Figures 4I–4K). Thus, PLAGL2 can drive intestinal epithelial growth and support stem cell potential despite severe Wnt depletion.

Oddly, despite the apparent augmentation of Wnt signaling by PLAGL2, TCF4/β-catenin target genes are not induced by PLAGL2 overexpression (Figure 5A). However, RNA-seq did reveal that ASCL2 target genes (as previously described by Schuijers et al., 2015) were modestly induced, in a dose-dependent manner, in PLAGL2-expressing enteroids (Figure 5A). RT-PCR for canonical Wnt target genes *Axin2* and *Cd44* confirmed no increase of these transcripts (Figure 5B). Expression analysis in both mouse (Figure 5C) and human (Figure 5D) organoids confirmed that PLAGL2 augments expression of *ASCL2*, in a dose-dependent manner. Using a gene set of ASCL2-induced transcripts (Schuijers et al., 2015) we compared PLAGL2-modulated transcripts using GSEA, which reveals enrichment of an ASCL2 signature in PLAGL2-upregulated genes (Figure 5E). Decreased expression of *Ascl2* and the ASCL2 target, *Lgr5*, in *Plagl2* null enteroids also suggests a positive role for PLAGL2 in supporting ASCL2 expression (Figure 5F).

Although *ASCL2* is a TCF4/β-catenin target gene (Giakountis et al., 2016; Schuijers et al., 2015) that could be activated by increased levels of Wnt ligands, we investigated a possible Wnt-independent relationship between *PLAGL2* and *ASCL2*. We looked first at available RNA-seq data for CRC tumors, which frequently possess Wnt-activating mutations. RNA-seq data from CRC tumors were parsed according to common Wnt-activating mutations (truncating mutations in *APC* or *AXIN2*, or missense mutations in *CTNNB1*). This revealed a strong relationship between *PLAGL2* and *ASCL2* expression, regardless of these hallmarks of aberrant canonical Wnt pathway activation (Figure 5G). We then examined this relationship in a CRC tumor cell line, DLD1, which has inactivating mutations in *APC*. Inactivation of the endogenous *PLAGL2* gene in DLD1 CRC cells (Figure S2) causes a stepwise loss of *ASCL2* mRNA (Figure 5H), suggesting dependency on PLAGL2, despite constitutive Wnt pathway activation in these cells. Thus, PLAGL2 is a necessary component of the regulatory mechanisms operating upstream of ASCL2.

We next examined whether the cell-autonomous defect in lineage tracing following mutagenesis of *Plagl2* (Figure 2O) could be rescued by ASCL2. In enteroids transfected with the stable gRNA transposon, we co-transfected an ASCL2-expressing transposon. ASCL2 rescued the lineage-tracing defect in *Plagl2*-mutated enteroids (Figure 5I). Both T7E1 assays (Figure 5J) and Illumina-based genotyping for the targeted region of *Plagl2* (Figure 5K) revealed similar levels of mutagenesis in both populations, but not enteroids targeted with a non-specific gRNA.

To investigate the importance of PLAGL2 in the transcriptional activation of *ASCL2*, we constructed a fluorescent reporter vector with the mouse *Ascl2* proximal promoter (Figure 6A). Assays in DLD1 cells revealed that constitutive expression of PLAGL2 augmented reporter activity (Figures 6B and 6C), while siRNA knockdown of endogenous PLAGL2 resulted in decreased activity (Figure 6D). To examine direct interaction, we employed chromatin immunoprecipitation (ChIP) to determine if PLAGL2 binds conserved PLAG consensus sites ($GRGGCN_{6\text{-}8}RGGK$, as previously defined by Hensen et al., 2002; Voz et al., 2000) located in the proximal mouse *Ascl2* promoter and near a 3′ lncRNA (*Wintrlinc1*) (Figure 6E). ChIP and qPCR revealed clear interaction of PLAGL2 with the *Ascl2* promoter in both PLAGL2-O/E enteroid clones (Figure 6F). ChIP also indicated interaction with the mouse *Wintrlinc1* promoter, although only in enteroids expressing higher levels of PLAGL2 (Figure 6F). Thus, PLAGL2 interacts with *cis* regulatory sequences near *ASCL2* and can drive transcription of the *ASCL2* promoter.

(O) Quantification of lineage-tracing events in stable $Cas9^{D10A}$-expressing enteroids 7 days after transfection with a transposon constitutively expressing gRNAs targeting *Plagl2* or *LacZ* (NS gRNA).
(P) Exemplary images of a lineage-tracing event from days 4 to 7 post-transfection (red arrow) described above, as observed via constitutive GFP co-expression from the gRNA-expressing transposon. Single isolated transfected cells (black arrowhead) that do not expand are not quantified as lineage-tracing events.
Student's one-tailed t test was performed to evaluate significance between means of replicates, where *$p < 0.05$ and **$p < 0.01$.

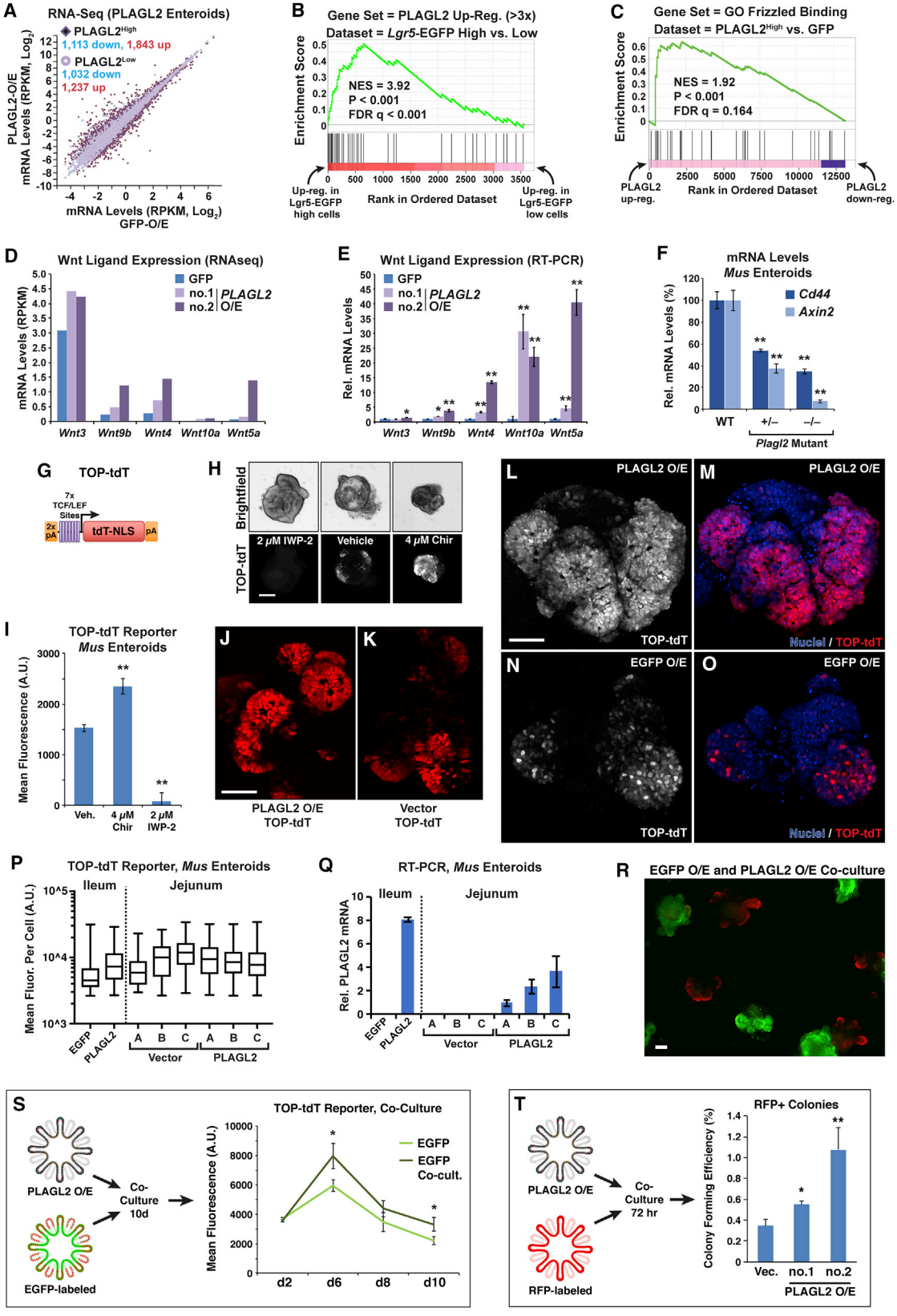

(legend on next page)

DISCUSSION

Here, we have reported the role for the transcription factor PLAGL2 in promoting stem cell identity, in part through direct transcriptional activation of *ASCL2*, which may be responsible for Wnt-independent growth driven by PLAGL2. Previously, known regulators of *ASCL2* in the intestine were limited to the Wnt pathway transcriptional activators TCF4/β-catenin (Schuijers et al., 2015) and *WiNTRLINC1*, a long non-coding RNA (lncRNA) located 3′ of *ASCL2* that is also needed for human *ASCL2* expression (Giakountis et al., 2016). The transcriptional activation of *WiNTRLINC1* by TCF4/β-catenin is coupled with the transcriptional activation of *ASCL2,* with the lncRNA itself aiding in chromatin looping between TCF4/β-catenin-bound *WiNTRLINC1* and the *ASCL2* promoter (Giakountis et al., 2016). While we do not observe any change of the mouse *Wintrlinc1* RNA in PLAGL2-expressing mouse enteroids (data not shown), the *Wintrlinc1* promoter itself may act in a facultative fashion as an enhancer for *ASCL2,* independent of the *Wintrlinc1* RNA. lncRNA promoters have been documented to execute this type of *cis* regulation of neighboring genes (Engreitz et al., 2016).

In vivo, a role for *PLAGL2* in stem cell development and/or homeostasis remains to be determined. Early in murine post-natal intestinal development (post-natal day 3, or p3) PLAGL2 protein appears to be distributed throughout epithelial cells along the crypt-villus axis, with mRNA levels dropping gradually after p14 (Van Dyck et al., 2007). While mice homozygous for a germline null mutation in *Plagl2* die shortly after birth, the reason for this mortality is unclear, and may be due to stem cell failure, or due to epithelial lipid malabsorption, as proposed previously (Van Dyck et al., 2007). *In vivo, Plagl2*-null phenotypes caused by depletion of Wnt ligand expression may be masked by the unperturbed expression of stromal-derived Wnts. A conditional (e.g., floxed) allele is needed to determine the role of PLAGL2 in the adult mouse intestinal epithelium through conditional inactivation.

In addition to direct regulation of ASCL2, PLAGL2 also appears to drive Wnt signaling, although this effect appears minimal in our overexpression model; i.e., Wnt target genes are not globally increased, and TOP-tdT reporter activity is only modestly increased. PLAGL2 O/E appears to augment the abundance of Wnt-high cells, as gauged from our confocal microscopy, which may reflect a compartmentalized effect of PLAGL2, perhaps only within the IESC lineage. The Wnt targets *Cd44* and *Axin2*, which are not restricted to the IESC lineage (Li et al., 2016; Zeilstra et al., 2014), may only be increased in IESCs, which could be obfuscated by expression analysis of total RNA from whole enteroids. Alternatively, in the context of overexpression, PLAGL2-mediated effects on canonical Wnt signaling may depend on limiting co-factors. This could account for depletion of Wnt targets in *Plagl2* knockouts, but not increased abundance of the same targets following PLAGL2 O/E. Previous

Figure 3. PLAGL2 Drives an Lgr5^{High} Intestinal Stem Cell Signature and Wnt Activation

(A) Scatterplot of reads per kilobase of transcript per million mapped reads (RPKM) values from RNA-seq of mouse enteroids, clone no. 1 (PLAGL2-Low O/E) and clone no. 2 (PLAGL2-High O/E), compared with GFP-expressing (GFP-TG) enteroids. The number of genes down- or upregulated >2-fold for each clone is indicated.

(B) GSEA using a gene set consisting of 600 transcripts upregulated >3-fold in PLAGL2 no. 2 enteroids, and upregulated >1.05-fold in PLAGL2 no. 1 enteroids, relative to GFP-TG enteroids. Dataset is a ranked list of 3,566 transcripts from Lgr5-EGFP-sorted IESCs selected for up- or downregulation, relative to Lgr5-EGFP^{LOW} cells ($p < 0.05$) from a published dataset (Munoz et al., 2012).

(C) GSEA against all molecular function gene ontology (GO) terms revealed a strong "Frizzled Binding" enrichment in the RNA-seq dataset.

(D) Expression levels of Wnt ligand genes altered by PLAGL2 O/E, represented as RPKM values from RNA-seq data.

(E) RT-PCR validation of Wnt mRNA levels, expressed relative to GFP controls.

(F) RT-PCR for the Wnt target genes *Cd44* and *Axin2* in WT and *Plagl2* mutant ileum enteroids.

(G) Schematic map of Tcf/Lef reporter (TOP-tdT) transposon that expresses tdTomato with a nuclear-localization signal (tdT-NLS).

(H and I) Representative images of stable lines of WT mouse enteroids with the TOP-tdT reporter treated for 48 hr with vehicle (0.1% DMSO), 4 μM Chir99021, or 2 μM IWP-2 (H), with fluorescence quantified in (I).

(J–O) Confocal image of TOP-tdT fluorescence in jejunum enteroid clone A stably overexpressing PLAGL2 (J), with empty vector control A depicted in (K). Confocal image of TOP-tdT fluorescence in ileum PLAGL2 O/E enteroid (L) (white), and overlaid in red with a nuclear stain (M). Control enteroids (GFP O/E) are shown in (N) and (O).

(P) Enteroids from eight independent *Piggybac* transgenic lines were dissociated for quantifying fluorescence in each cell.

(Q) RT-PCR for the human PLAGL2 cDNA expressed in mouse ileum and jejunum enteroid lines, also transgenic for TOP-tdT.

(R) Images of GFP-labeled and PLAGL2 O/E ileum enteroids co-cultured together for 10 days.

(S) Enteroids overexpressing PLAGL2 or GFP were imaged for TOP-tdT reporter activity following 10 days of culture, with increased reporter activity evident in GFP-expressing enteroids co-cultured with PLAGL2-expressing enteroids.

(T) PLAGL2 O/E enhances colony-forming potential of RFP-expressing (*ROSA26^{mTmG}*) WT mouse enteroids following 72 hr of co-culture. Scale bars, 50 μm. Student's one-tailed t test was performed to evaluate significance between means of replicates, where $*p < 0.05$ and $**p < 0.01$.

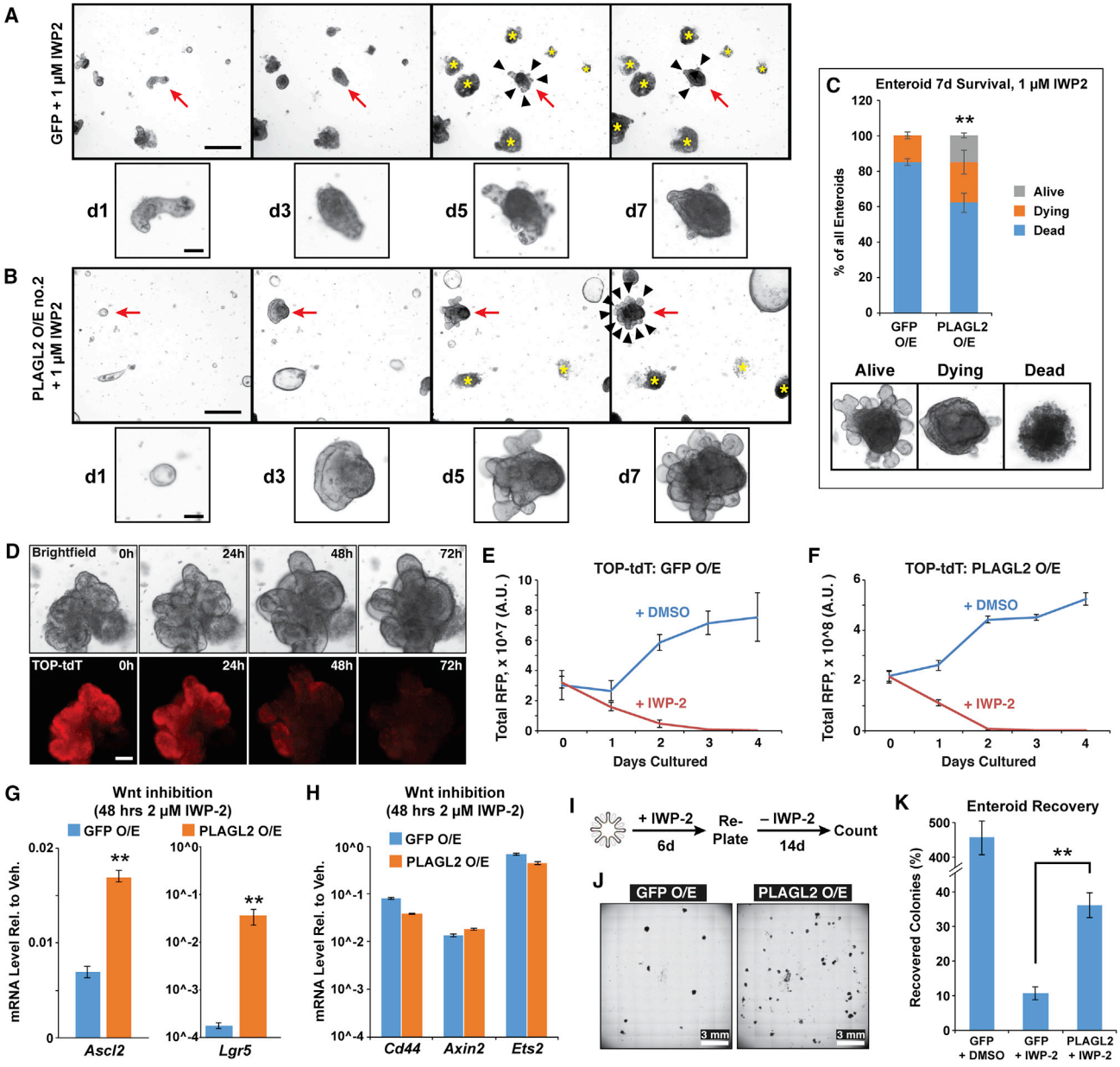

Figure 4. PLAGL2 Drives Enteroid Growth and Survival in the Absence of Wnt

(A and B) GFP-expressing (A) or PLAGL2-O/E (B) enteroids were plated in ENR medium containing DMSO or 1 μM IWP2 and monitored over 7 days for viability. The vast majority of GFP-expressing enteroids are dead by 5 days with 1 μM IWP2 treatment (A) (yellow asterisks) while rare surviving enteroids begin to regress by day 7 (A) (red arrow, and inset). Many PLAGL2-O/E enteroids survive 1 μM IWP2, mostly as cysts, with some persisting as budding enteroids (B) (red arrow, and inset). Enteroid buds are indicated with arrowheads, and yellow asterisks indicate dead enteroids.

(C) Quantification of surviving enteroids following 7 days of IWP-2 treatment, with morphological qualification of status (see Supplemental Experimental Procedures).

(D–F) Representative images of a TOP-tdT enteroid, overexpressing PLAGL2, imaged over 72 hr of treatment with 2 μM IWP-2 (D). Levels of tdT were quantified in enteroids expressing either GFP (E) or PLAGL2 (F) over 4 days of treatment, after which tdT fluorescence was not visible in any organoid treated with IWP-2.

(G) RT-PCR for stem cell markers *Ascl2* and *Lgr5* in TOP-tdT enteroids treated with 2 μM IWP-2 for 48 hr, relative to levels in enteroids treated with 0.1% DMSO (Veh.).

(H) RT-PCR for Wnt target genes, as in (G).

(legend continued on next page)

effects of PLAGL2 on Wnt ligand expression have also been documented in glioma cells, although PLAGL2 drives expression of Wnt6 in this model (Zheng et al., 2010). The involvement of other PLAGL2 targets also cannot currently be excluded as possible modulators of Wnt signaling.

It is rather enigmatic that PLAGL2 robustly induces the expression of Wnt genes (*Wnt9b, Wnt4, Wnt10a,* and *Wnt5a*) when overexpressed in enteroids, yet modestly augments canonical Wnt signaling. These Wnts may be minor components compared with the larger pool of Wnt3 (or Wnt2b, *in vivo*). In addition, robust *Wnt4* and *Wnt5a* induction by PLAGL2 may trigger the activation of non-canonical Wnt signaling. These Wnts can activate non-canonical Wnt signaling pathways (Heinonen et al., 2011; Tanigawa et al., 2011; Wallingford et al., 2001; Yamanaka et al., 2002) and antagonize canonical signaling, which is observed for both Wnt5a (Bernard et al., 2008; Topol et al., 2003; Yuzugullu et al., 2009) and Wnt4 (Bernard et al., 2008; Tanaka et al., 2011). In CRC, *WNT5A* is frequently downregulated, antagonizes canonical Wnt signaling, represses epithelial-to-mesenchymal transition, and slows CRC cell line proliferation (Cheng et al., 2014). Consistent with this, Wnt5a is a stromal signal that antagonizes epithelial proliferation of wounded mucosa in the mouse colon but is necessary for regeneration (Miyoshi et al., 2012). More studies of the roles of each Wnt ligand are needed for the colon, which appears more resistant to loss of all Wnt ligands, as observed following global inactivation of Wntless (*Wls*) in the mouse (Farin et al., 2012). PLAGL2 may have differing effects in these compartments (colon versus small intestine), *in vivo*, perhaps due to unique contexts of specific Wnt ligands.

In future efforts to antagonize canonical Wnt signaling in CRC tumors for therapeutic purposes, as underway in mouse models (Cha and Choi, 2016; Fang et al., 2016; Masuda et al., 2016; Qu et al., 2016; Yamada and Masuda, 2017), it may be necessary to consider pathways that drive Wnt-independent maintenance of proliferation or a stem cell-like state. PLAGL2 appears to drive such a pathway and may also be a relevant target for therapeutic inhibition.

EXPERIMENTAL PROCEDURES

Vector Construction

BII-ChPt and BII-ChBt vectors for Piggybac-mediated transgenesis were constructed using standard molecular cloning techniques. PLAGL2 was PCR amplified and cloned, in frame, between each BsmBI restriction site (see Supplemental Information). LIN28B was cloned into the PB533A-2 vector (System Biosciences) between the XbaI and SwaI restriction sites after PCR amplification from the MSCV-PIG-LIN28B vector (King et al., 2011). The pCMV-hyPBase plasmid (Yusa et al., 2011) was a gift from Allan Bradley (Wellcome Trust Sanger Institute).

Transgenic Organoid Production

Human organoids were established from biopsies obtained from healthy patients undergoing routine colonoscopy, cultured as described previously (Matano et al., 2015), and transfected with the PB533A-LIN28B (transfected at passage 8) or BII-ChBt-PLAGL2 (transfected at passage 10) using previously described protocols (Fujii et al., 2015).

Mouse jejunum enteroids established from 6- to 8-week-old C57BL/6 mice were transfected with the BII-ChPt-PLAGL2 or -GFP *Piggybac* transposons at passage 3. Enteroids were transfected with 1 μg DNA (200 ng pCMV-hyPBase, 800 ng BII-ChPt-PLAGL2, or BII-ChPt-GFP) by spinoculation as described previously (Schwank et al., 2013) using lipofectamine 2000 (Thermo Fisher Scientific). All experiments for human or mouse organoids (transgenic, knockout, or WT) were performed between passages 4 and 12.

RNA Isolation and RT-PCR

Cells/enteroids were homogenized in 1.0 mL TRIzol (Thermo Fisher Scientific) for 30–45 s using a BeadBug homogenizer (Benchmark Scientific), and total RNA isolated per the manufacturer's specifications. RT reactions were performed with oligo(dT) primers using 1–4 μg RNA and Superscript III (Thermo Fisher Scientific). qPCR was achieved with Bullseye EvaGreen qPCR MasterMix (MIDSCI) using primers in Table S2.

Colony-Forming Assays

For human organoid colony-forming assays, organoids were dissociated in TrypLE Express (Thermo Fisher Scientific) containing 250 U/mL DNase I and 10 μM Y27632 for 20 min at 37°C. Single cells were plated in quadruplicate at 5,000 cells/well on a 24-well plate. Images were taken and quantified at day 0 and day 7 (LIN28B organoids) or day 10 (PLAGL2 organoids) using the BioTek Cytation 3 Imaging Platform. Mouse enteroids were also dissociated with TrypLE, for 5 min, and plated/imaged as above.

Mutagenesis of Plagl2 in Mouse Enteroids

For generating knockouts of mouse *Plagl2* C57BL/6 jejunum and ileum enteroids (from 6- to 8-week-old mice, each at passage no. 1) were expanded for transfection as described above. Enteroids were dissociated into single cells with TrypLE (Thermo Fisher Scientific) and transfected with Cas9 plasmids, pCMV-hyPBase, and BII-ChPtG. Transfectants were selected with 2 μg/mL puromycin and picked after 7 days.

(I and J) TOP-tdT enteroids were treated 6 days with 2 μM IWP-2 and then 14 days in complete ENR medium (I), followed by microscopic imaging (J).

(K) Quantification of enteroids from (J), relative to the original numbers of enteroid colonies present prior to IWP-2 treatment.

Scale bars, 50 μm. Student's one-tailed t tests were performed to evaluate significance between means of replicates, where *$p < 0.05$ and **$p < 0.01$.

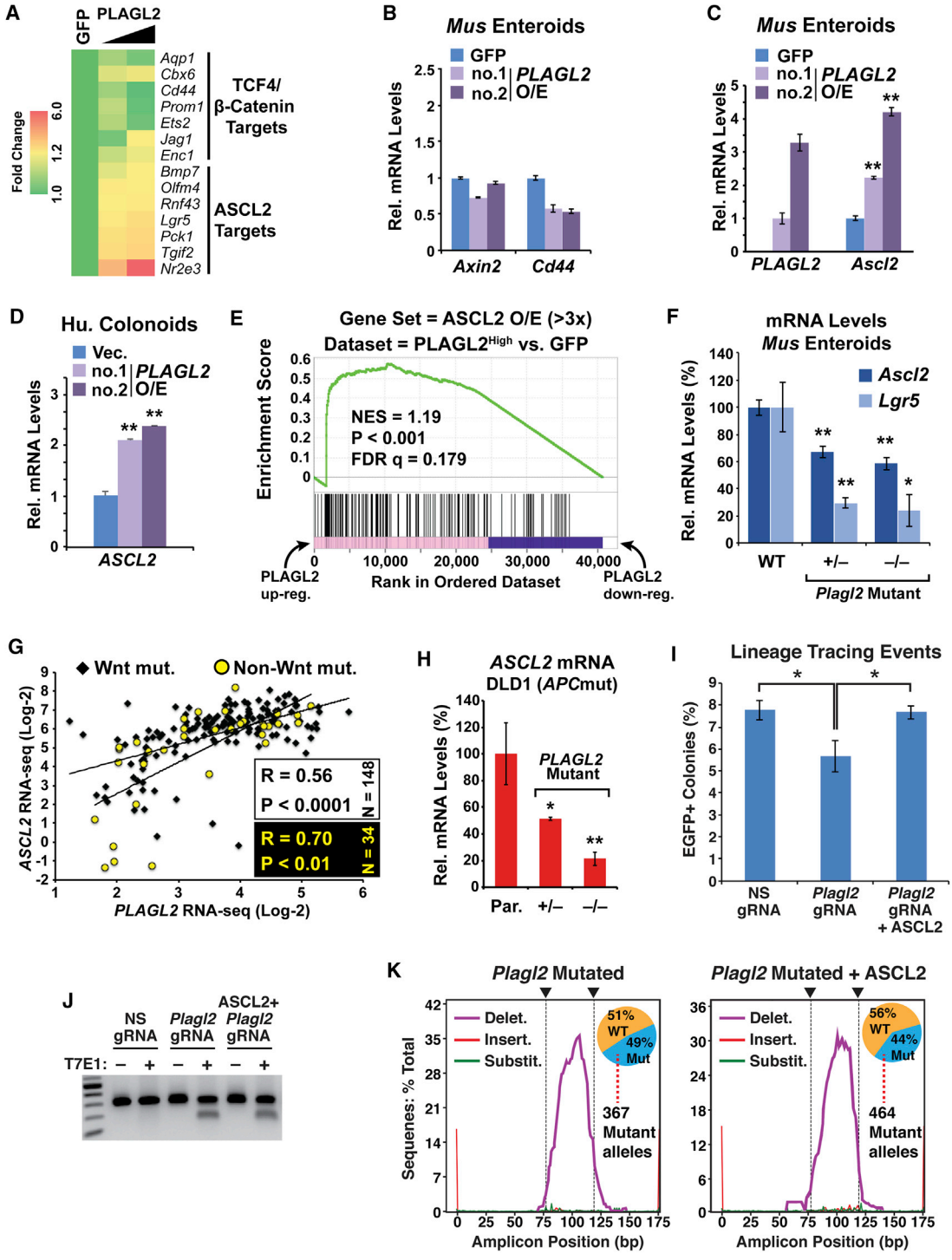

Figure 5. PLAGL2 Enhances *ASCL2* Expression, Independent of Canonical Wnt Signaling

(A–C) Heatmap reflecting RNA-seq data from clone no. 1 (PLAGL2-Low O/E, middle column) and clone no. 2 (PLAGL2-High O/E, right column) showing expression changes of TCF4/β-catenin and ASCL2 transcriptional targets relative to GFP control (A). RT-PCR was performed for canonical Wnt target genes, *Axin2* and *Cd44* (B), human *PLAGL2* and *Ascl2* (C) in mouse enteroids, clones no. 1 and 2.

(D) RT-PCR for *ASCL2* in human PLAGL2-O/E colonoids.

(E) GSEA against a gene set of mRNAs induced upon Ascl2 overexpression (Schuijers et al., 2015) revealed enrichment in the PLAGL2 RNA-seq dataset (clone no. 2).

(legend continued on next page)

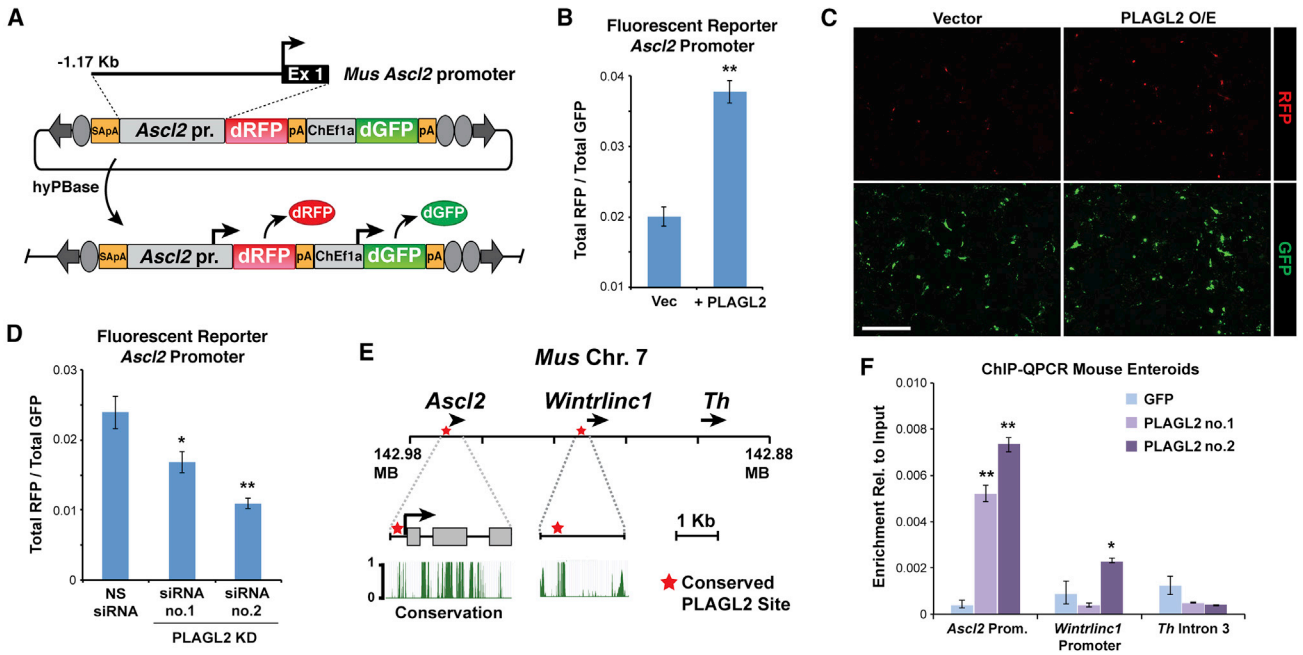

Figure 6. PLAGL2 Activates Transcription of the Mouse *Ascl2* Promoter and Directly Binds Sites near *Ascl2*

(A) Reporter transposon construct for measuring *Ascl2* promoter activity.

(B) *Ascl2* promoter activity as measured in DLD1 cells, after co-transfection with PLAGL2 expression construct or empty vector.

(C) Images of RFP and GFP fluorescent DLD1 cells from (B).

(D) siRNA knockdown of endogenous PLAGL2 in DLD1 cells following stable integration of the Ascl2 promoter reporter, pictured in (A). Reporter activity was measured 72 hr after siRNA transfection.

(E) Map of mouse chromosome 7 showing locations of *Ascl2, Wntrlinc1,* and *Th* genes and sites where two conserved PLAGL2 consensus sequences ($GRGGCN_{6\text{-}8}RGGK$) are located.

(F) Chromatin immunoprecipitation and qPCR for sequences encompassing these sites using lysates from PLAGL2 O/E (clones no. 1 and 2) and GFP-expressing mouse enteroids. Sequences within *Th* intron 3 were amplified as negative controls.

Scale bar, 500 μm. Student's one-tailed t test was performed to evaluate significance between means of replicates, where $*p < 0.05$ and $**p < 0.01$.

Transient Mutagenesis of *Plagl2* and Lineage Tracing in Mouse Enteroids

Mouse enteroids were first transfected and selected for stable expression of the Cas9 nuclease. This line of Cas9-expressing enteroids was then transfected with a *Piggybac* transposon driving constitutive expression of specific gRNAs and GFP. GFP expression and lineage-tracing events were imaged on days 4–7 after transfection, and lineage-tracing events quantified.

IWP2 Treatment of PLAGL2 Mouse Enteroids

BII-ChPt-PLAGL2 mouse enteroids were plated onto a 12-well plate (Greiner) in ENR-containing vehicle (0.1% DMSO), or the Wnt

(F) RT-PCR for *Ascl2* and *Lgr5* in mouse *Plagl2* mutant enteroids.

(G) RNA-seq data of one TCGA CRC patient cohort (N = 182), with tumors stratified according to activating Wnt pathway mutations (missense mutations in *CTNNB1* or truncating mutations in *APC* or *AXIN2*).

(H) RT-PCR for *ASCL2* in DLD1 CRC cells with *PLAGL2* heterozygous or homozygous null mutations.

(I) Quantification of lineage-tracing events in stable $Cas9^{D10A}$-expressing mouse enteroids 7 days after transfection with a transposon expressing gRNAs against *Plagl2*, and co-transfected for stable constitutive expression of ASCL2 (conferring blasticidin resistance).

(J) T7E1 assay of PCR products from the targeted (exon 3) region of *Plagl2* from blasticidin-resistant enteroids from (I).

(K) Illumina sequencing of targeted region of *Plagl2* from enteroids in (I) confirms mutagenesis of *Plagl2*, with vast majority of mutations consisting of insertions or deletions (indels). Targeted region in *Plagl2* amplicon by each unique gRNA (for paired nickase with $Cas9^{D10A}$) is indicated with arrowheads.

Student's one- or two-tailed t test was performed to evaluate significance between means of replicates, where $*p < 0.05$ and $**p < 0.01$. See also Figures S1 and S2.

inhibitor, IWP-2 (Selleckchem) at 1 or 2 μM. Medium was changed every 48 hr. Enteroids were imaged daily for 7 days using a BioTek Cytation 3 Imaging Platform with Gen5 software to monitor enteroid viability.

Transfection with siRNA (for Knockdown) or miRNA Mimics

Transient transfection of DLD1 cells with the Let-7b mimic (IDT) was performed as follows. A total of 5×10^5 cells was plated in a six-well plate and transfected the next day with 1.25 μL of 20 μM miRNAs using the Lipofectamine RNAiMAX (Thermo Fisher Scientific) transfection reagent according to the manufacturer's instructions at a final concentration of 10 nM. After 72 hr, cells were homogenized in TRIzol and RNA isolated for RT-PCR.

mRNA-Seq

Data from these mRNA-seq experiments are available at the GEO at the NIH under accession number GEO: GSE115532.

Vertebrate Animals

Mouse models used in this study conform to standards of care and ethical treatment as determined by the Washington University Institutional Animal Care and Use Committee. The investigators sought and received approval for animal protocols in this study.

Statistical Methods

Statistical considerations are given for a parallel study of two groups, for pairwise comparison of two conditions, genotypes, or treatments. For comparison of two groups in a parallel design, performed in triplicate, we have a 90% likelihood of detecting a significant difference ($p < 0.05$) between groups if the true difference is 2.95 times the SD. This power calculation uses the non-central t-function distribution. Pairwise comparisons use Student's t test, either one- or two-tailed, depending on the initial hypothesis. Assays were performed three times for each experiment, in triplicate or quadruplicate. Data are represented as the mean, with error bars depicting the SEM.

SUPPLEMENTAL INFORMATION

Supplemental Information includes Supplemental Experimental Procedures, two figures, and three tables and can be found with this article online at https://doi.org/10.1016/j.stemcr.2018.06.009.

AUTHOR CONTRIBUTIONS

B.B.M. designed all DNA constructs, which were generated with assistance from T.P. A.M.S. and D.A.V.P. performed organoid cultures, including maintenance, colony-forming assays, and other manipulations. B.B.M. generated PLAGL2-overexpressing mouse enteroids, *Plagl2* knockout enteroids, TOP-tdT enteroids, and LIN28B-overexpressing human organoids, with assistance from A.M.S. and D.A.V.P. A.M.S. generated PLAGL2-overexpressing human organoids. B.B.M. performed all experiments in Figures 1 and 6, with assistance from L.D. for Let-7 reporter construction. B.B.M. prepared RNA for mRNA-seq and performed GSEA and all analysis of TCGA data. T.Z. generated PLAGL2-null DLD1 cell lines. P.O.B. and J.A.J.F. performed confocal microscopy analysis of TOP-tdT-expressing organoids, with assistance from D.A.V.P.

ACKNOWLEDGMENTS

B.B.M. is supported by grants from the NIH/NIDDK (DK093885, DK108764, and DK052574), the Siteman Cancer Center, and the Cancer Research Foundation (Young Investigator Award). Confocal and super-resolution image data were generated on a Zeiss LSM 880 Airyscan Confocal Microscope, which was purchased with support from the Office of Research Infrastructure Programs (ORIP), a part of the NIH Office of the Director under grant OD021629 to J.A.J.F. P.O.B. and J.A.J.F. would also like to gratefully acknowledge support from the Washington University Center for Cellular Imaging (WUCCI), which is supported in part by the Washington University School of Medicine, The Children's Discovery Institute of Washington University and St. Louis Children's Hospital (CDI-CORE-2015-505), and the Foundation for Barnes-Jewish Hospital (3770).

Received: October 20, 2017
Revised: June 11, 2018
Accepted: June 12, 2018
Published: July 12, 2018

REFERENCES

Barker, N., van Es, J.H., Kuipers, J., Kujala, P., van den Born, M., Cozijnsen, M., Haegebarth, A., Korving, J., Begthel, H., Peters, P.J., et al. (2007). Identification of stem cells in small intestine and colon by marker gene Lgr5. Nature *449*, 1003–1007.

Bernard, P., Fleming, A., Lacombe, A., Harley, V.R., and Vilain, E. (2008). Wnt4 inhibits beta-catenin/TCF signalling by redirecting beta-catenin to the cell membrane. Biol. Cell *100*, 167–177.

Buczacki, S.J., Zecchini, H.I., Nicholson, A.M., Russell, R., Vermeulen, L., Kemp, R., and Winton, D.J. (2013). Intestinal label-retaining cells are secretory precursors expressing Lgr5. Nature *495*, 65–69.

Carvalho, B., Postma, C., Mongera, S., Hopmans, E., Diskin, S., van de Wiel, M.A., van Criekinge, W., Thas, O., Matthai, A., Cuesta, M.A., et al. (2009). Multiple putative oncogenes at the chromosome 20q amplicon contribute to colorectal adenoma to carcinoma progression. Gut *58*, 79–89.

Cha, P.H., and Choi, K.Y. (2016). Simultaneous destabilization of beta-catenin and Ras via targeting of the axin-RGS domain as a potential therapeutic strategy for colorectal cancer. BMB Rep. *49*, 455–456.

Chen, B., Dodge, M.E., Tang, W., Lu, J., Ma, Z., Fan, C.W., Wei, S., Hao, W., Kilgore, J., Williams, N.S., et al. (2009). Small molecule-mediated disruption of Wnt-dependent signaling in tissue regeneration and cancer. Nat. Chem. Biol. *5*, 100–107.

Cheng, R., Sun, B., Liu, Z., Zhao, X., Qi, L., Li, Y., and Gu, Q. (2014). Wnt5a suppresses colon cancer by inhibiting cell proliferation and epithelial-mesenchymal transition. J. Cell. Physiol. *229*, 1908–1917.

Copley, M.R., Babovic, S., Benz, C., Knapp, D.J., Beer, P.A., Kent, D.G., Wohrer, S., Treloar, D.Q., Day, C., Rowe, K., et al. (2013). The Lin28b-let-7-Hmga2 axis determines the higher self-renewal potential of fetal haematopoietic stem cells. Nat. Cell Biol. *15*, 916–925.

de Lau, W., Barker, N., Low, T.Y., Koo, B.K., Li, V.S., Teunissen, H., Kujala, P., Haegebarth, A., Peters, P.J., van de Wetering, M., et al. (2011). Lgr5 homologues associate with Wnt receptors and mediate R-spondin signalling. Nature *476*, 293–297.

Engreitz, J.M., Haines, J.E., Perez, E.M., Munson, G., Chen, J., Kane, M., McDonel, P.E., Guttman, M., and Lander, E.S. (2016). Local regulation of gene expression by lncRNA promoters, transcription and splicing. Nature *539*, 452–455.

Fang, L., Zhu, Q., Neuenschwander, M., Specker, E., Wulf-Goldenberg, A., Weis, W.I., von Kries, J.P., and Birchmeier, W. (2016). A small-molecule antagonist of the beta-catenin/TCF4 interaction blocks the self-renewal of cancer stem cells and suppresses tumorigenesis. Cancer Res. *76*, 891–901.

Farin, H.F., Van Es, J.H., and Clevers, H. (2012). Redundant sources of Wnt regulate intestinal stem cells and promote formation of Paneth cells. Gastroenterology *143*, 1518–1529.e7.

Fujii, M., Matano, M., Nanki, K., and Sato, T. (2015). Efficient genetic engineering of human intestinal organoids using electroporation. Nat. Protoc. *10*, 1474–1485.

Giakountis, A., Moulos, P., Zarkou, V., Oikonomou, C., Harokopos, V., Hatzigeorgiou, A.G., Reczko, M., and Hatzis, P. (2016). A positive regulatory loop between a Wnt-regulated non-coding RNA and ASCL2 controls intestinal stem cell fate. Cell Rep. *15*, 2588–2596.

Hagan, J.P., Piskounova, E., and Gregory, R.I. (2009). Lin28 recruits the TUTase Zcchc11 to inhibit let-7 maturation in mouse embryonic stem cells. Nat. Struct. Mol. Biol. *16*, 1021–1025.

He, Q.J., Zeng, W.F., Sham, J.S., Xie, D., Yang, X.W., Lin, H.L., Zhan, W.H., Lin, F., Zeng, S.D., Nie, D., et al. (2003). Recurrent genetic alterations in 26 colorectal carcinomas and 21 adenomas from Chinese patients. Cancer Genet. Cytogenet. *144*, 112–118.

Heinonen, K.M., Vanegas, J.R., Lew, D., Krosl, J., and Perreault, C. (2011). Wnt4 enhances murine hematopoietic progenitor cell expansion through a planar cell polarity-like pathway. PLoS One *6*, e19279.

Hensen, K., Van Valckenborgh, I.C., Kas, K., Van de Ven, W.J., and Voz, M.L. (2002). The tumorigenic diversity of the three PLAG family members is associated with different DNA binding capacities. Cancer Res. *62*, 1510–1517.

Heo, I., Joo, C., Cho, J., Ha, M., Han, J., and Kim, V.N. (2008). Lin28 mediates the terminal uridylation of let-7 precursor MicroRNA. Mol. Cell *32*, 276–284.

Hermsen, M., Postma, C., Baak, J., Weiss, M., Rapallo, A., Sciutto, A., Roemen, G., Arends, J.W., Williams, R., Giaretti, W., et al. (2002). Colorectal adenoma to carcinoma progression follows multiple pathways of chromosomal instability. Gastroenterology *123*, 1109–1119.

King, C.E., Wang, L., Winograd, R., Madison, B.B., Mongroo, P.S., Johnstone, C.N., and Rustgi, A.K. (2011). LIN28B fosters colon cancer migration, invasion and transformation through let-7-dependent and -independent mechanisms. Oncogene *30*, 4185–4193.

Korinek, V., Barker, N., Moerer, P., van Donselaar, E., Huls, G., Peters, P.J., and Clevers, H. (1998). Depletion of epithelial stem-cell compartments in the small intestine of mice lacking Tcf-4. Nat. Genet. *19*, 379–383.

Lee, R.C., and Ambros, V. (2001). An extensive class of small RNAs in *Caenorhabditis elegans*. Science *294*, 862–864.

Li, N., Yousefi, M., Nakauka-Ddamba, A., Jain, R., Tobias, J., Epstein, J.A., Jensen, S.T., and Lengner, C.J. (2014). Single-cell analysis of proxy reporter allele-marked epithelial cells establishes intestinal stem cell hierarchy. Stem Cell Rep. *3*, 876–891.

Li, N., Yousefi, M., Nakauka-Ddamba, A., Tobias, J.W., Jensen, S.T., Morrisey, E.E., and Lengner, C.J. (2016). Heterogeneity in readouts of canonical wnt pathway activity within intestinal crypts. Dev. Dyn. *245*, 822–833.

Madison, B.B., Liu, Q., Zhong, X., Hahn, C.M., Lin, N., Emmett, M.J., Stanger, B.Z., Lee, J.S., and Rustgi, A.K. (2013). LIN28B promotes growth and tumorigenesis of the intestinal epithelium via Let-7. Genes Dev. *27*, 2233–2245.

Madison, B.B., Jeganathan, A.N., Mizuno, R., Winslow, M.M., Castells, A., Cuatrecasas, M., and Rustgi, A.K. (2015). Let-7 represses carcinogenesis and a stem cell phenotype in the intestine via regulation of Hmga2. PLoS Genet. *11*, e1005408.

Masuda, M., Uno, Y., Ohbayashi, N., Ohata, H., Mimata, A., Kukimoto-Niino, M., Moriyama, H., Kashimoto, S., Inoue, T., Goto, N., et al. (2016). TNIK inhibition abrogates colorectal cancer stemness. Nat. Commun. *7*, 12586.

Matano, M., Date, S., Shimokawa, M., Takano, A., Fujii, M., Ohta, Y., Watanabe, T., Kanai, T., and Sato, T. (2015). Modeling colorectal cancer using CRISPR-Cas9-mediated engineering of human intestinal organoids. Nat. Med. *21*, 256–262.

Miyoshi, H., Ajima, R., Luo, C.T., Yamaguchi, T.P., and Stappenbeck, T.S. (2012). Wnt5a potentiates TGF-beta signaling to promote colonic crypt regeneration after tissue injury. Science *338*, 108–113.

Munoz, J., Stange, D.E., Schepers, A.G., van de Wetering, M., Koo, B.K., Itzkovitz, S., Volckmann, R., Kung, K.S., Koster, J., Radulescu, S., et al. (2012). The Lgr5 intestinal stem cell signature: robust expression of proposed quiescent '+4' cell markers. EMBO J. *31*, 3079–3091.

Oshima, M., Hasegawa, N., Mochizuki-Kashio, M., Muto, T., Miyagi, S., Koide, S., Yabata, S., Wendt, G.R., Saraya, A., Wang, C., et al. (2016). Ezh2 regulates the Lin28/let-7 pathway to restrict activation of fetal gene signature in adult hematopoietic stem cells. Exp. Hematol. *44*, 282–296.e3.

Pinto, D., Gregorieff, A., Begthel, H., and Clevers, H. (2003). Canonical Wnt signals are essential for homeostasis of the intestinal epithelium. Genes Dev. *17*, 1709–1713.

Piskounova, E., Viswanathan, S.R., Janas, M., LaPierre, R.J., Daley, G.Q., Sliz, P., and Gregory, R.I. (2008). Determinants of microRNA processing inhibition by the developmentally regulated RNA-binding protein Lin28. J. Biol. Chem. *283*, 21310–21314.

Qu, Y., Gharbi, N., Yuan, X., Olsen, J.R., Blicher, P., Dalhus, B., Brokstad, K.A., Lin, B., Oyan, A.M., Zhang, W., et al. (2016).

Axitinib blocks Wnt/beta-catenin signaling and directs asymmetric cell division in cancer. Proc. Natl. Acad. Sci. USA *113*, 9339–9344.

Rahkonen, N., Stubb, A., Malonzo, M., Edelman, S., Emani, M.R., Narva, E., Lahdesmaki, H., Ruohola-Baker, H., Lahesmaa, R., and Lund, R. (2016). Mature Let-7 miRNAs fine tune expression of LIN28B in pluripotent human embryonic stem cells. Stem Cell Res. *17*, 498–503.

Rowe, R.G., Wang, L.D., Coma, S., Han, A., Mathieu, R., Pearson, D.S., Ross, S., Sousa, P., Nguyen, P.T., Rodriguez, A., et al. (2016). Developmental regulation of myeloerythroid progenitor function by the Lin28b-let-7-Hmga2 axis. J. Exp. Med. *213*, 1497–1512.

Rybak, A., Fuchs, H., Smirnova, L., Brandt, C., Pohl, E.E., Nitsch, R., and Wulczyn, F.G. (2008). A feedback loop comprising lin-28 and let-7 controls pre-let-7 maturation during neural stem-cell commitment. Nat. Cell Biol. *10*, 987–993.

Sabates-Bellver, J., Van der Flier, L.G., de Palo, M., Cattaneo, E., Maake, C., Rehrauer, H., Laczko, E., Kurowski, M.A., Bujnicki, J.M., Menigatti, M., et al. (2007). Transcriptome profile of human colorectal adenomas. Mol. Cancer Res. *5*, 1263–1275.

Sangiorgi, E., and Capecchi, M.R. (2008). Bmi1 is expressed in vivo in intestinal stem cells. Nat. Genet. *40*, 915–920.

Sato, T., van Es, J.H., Snippert, H.J., Stange, D.E., Vries, R.G., van den Born, M., Barker, N., Shroyer, N.F., van de Wetering, M., and Clevers, H. (2011). Paneth cells constitute the niche for Lgr5 stem cells in intestinal crypts. Nature *469*, 415–418.

Schuijers, J., Junker, J.P., Mokry, M., Hatzis, P., Koo, B.K., Sasselli, V., van der Flier, L.G., Cuppen, E., van Oudenaarden, A., and Clevers, H. (2015). Ascl2 acts as an R-spondin/Wnt-responsive switch to control stemness in intestinal crypts. Cell Stem Cell *16*, 158–170.

Schwank, G., Andersson-Rolf, A., Koo, B.K., Sasaki, N., and Clevers, H. (2013). Generation of BAC transgenic epithelial organoids. PLoS One *8*, e76871.

Slack, F.J., Basson, M., Liu, Z., Ambros, V., Horvitz, H.R., and Ruvkun, G. (2000). The lin-41 RBCC gene acts in the *C. elegans* heterochronic pathway between the let-7 regulatory RNA and the LIN-29 transcription factor. Mol. Cell *5*, 659–669.

Subramanian, A., Tamayo, P., Mootha, V.K., Mukherjee, S., Ebert, B.L., Gillette, M.A., Paulovich, A., Pomeroy, S.L., Golub, T.R., Lander, E.S., et al. (2005). Gene set enrichment analysis: a knowledge-based approach for interpreting genome-wide expression profiles. Proc. Natl. Acad. Sci. USA *102*, 15545–15550.

Takeda, N., Jain, R., LeBoeuf, M.R., Wang, Q., Lu, M.M., and Epstein, J.A. (2011). Interconversion between intestinal stem cell populations in distinct niches. Science *334*, 1420–1424.

Tanaka, S., Terada, K., and Nohno, T. (2011). Canonical Wnt signaling is involved in switching from cell proliferation to myogenic differentiation of mouse myoblast cells. J. Mol. Signal. *6*, 12.

Tanigawa, S., Wang, H., Yang, Y., Sharma, N., Tarasova, N., Ajima, R., Yamaguchi, T.P., Rodriguez, L.G., and Perantoni, A.O. (2011). Wnt4 induces nephronic tubules in metanephric mesenchyme by a non-canonical mechanism. Dev. Biol. *352*, 58–69.

Tian, H., Biehs, B., Warming, S., Leong, K.G., Rangell, L., Klein, O.D., and de Sauvage, F.J. (2011). A reserve stem cell population in small intestine renders Lgr5-positive cells dispensable. Nature *478*, 255–259.

Topol, L., Jiang, X., Choi, H., Garrett-Beal, L., Carolan, P.J., and Yang, Y. (2003). Wnt-5a inhibits the canonical Wnt pathway by promoting GSK-3-independent beta-catenin degradation. J. Cell Biol. *162*, 899–908.

Tran, N.D., Kissner, M., Subramanyam, D., Parchem, R.J., Laird, D.J., and Blelloch, R.H. (2016). A miR-372/let-7 axis regulates human germ versus somatic cell fates. Stem Cells *34*, 1985–1991.

Tu, H.C., Schwitalla, S., Qian, Z., LaPier, G.S., Yermalovich, A., Ku, Y.C., Chen, S.C., Viswanathan, S.R., Zhu, H., Nishihara, R., et al. (2015). LIN28 cooperates with WNT signaling to drive invasive intestinal and colorectal adenocarcinoma in mice and humans. Genes Dev. *29*, 1074–1086.

Uronis, J.M., Osada, T., McCall, S., Yang, X.Y., Mantyh, C., Morse, M.A., Lyerly, H.K., Clary, B.M., and Hsu, D.S. (2012). Histological and molecular evaluation of patient-derived colorectal cancer explants. PLoS One *7*, e38422.

van der Flier, L.G., van Gijn, M.E., Hatzis, P., Kujala, P., Haegebarth, A., Stange, D.E., Begthel, H., van den Born, M., Guryev, V., Oving, I., et al. (2009). Transcription factor achaete scute-like 2 controls intestinal stem cell fate. Cell *136*, 903–912.

Van Dyck, F., Braem, C.V., Chen, Z., Declercq, J., Deckers, R., Kim, B.M., Ito, S., Wu, M.K., Cohen, D.E., Dewerchin, M., et al. (2007). Loss of the PlagL2 transcription factor affects lacteal uptake of chylomicrons. Cell Metab. *6*, 406–413.

Viswanathan, S.R., Daley, G.Q., and Gregory, R.I. (2008). Selective blockade of microRNA processing by Lin28. Science *320*, 97–100.

Voz, M.L., Agten, N.S., Van de Ven, W.J., and Kas, K. (2000). PLAG1, the main translocation target in pleomorphic adenoma of the salivary glands, is a positive regulator of IGF-II. Cancer Res. *60*, 106–113.

Wallingford, J.B., Vogeli, K.M., and Harland, R.M. (2001). Regulation of convergent extension in *Xenopus* by Wnt5a and Frizzled-8 is independent of the canonical Wnt pathway. Int. J. Dev. Biol. *45*, 225–227.

West, J.A., Viswanathan, S.R., Yabuuchi, A., Cunniff, K., Takeuchi, A., Park, I.H., Sero, J.E., Zhu, H., Perez-Atayde, A., Frazier, A.L., et al. (2009). A role for Lin28 in primordial germ-cell development and germ-cell malignancy. Nature *460*, 909–913.

Yamada, T., and Masuda, M. (2017). Emergence of TNIK inhibitors in cancer therapeutics. Cancer Sci. *108*, 818–823.

Yamanaka, H., Moriguchi, T., Masuyama, N., Kusakabe, M., Hanafusa, H., Takada, R., Takada, S., and Nishida, E. (2002). JNK functions in the non-canonical Wnt pathway to regulate convergent extension movements in vertebrates. EMBO Rep. *3*, 69–75.

Yan, K.S., Chia, L.A., Li, X., Ootani, A., Su, J., Lee, J.Y., Su, N., Luo, Y., Heilshorn, S.C., Amieva, M.R., et al. (2012). The intestinal stem cell markers Bmi1 and Lgr5 identify two functionally distinct populations. Proc. Natl. Acad. Sci. USA *109*, 466–471.

Yan, K.S., Janda, C.Y., Chang, J., Zheng, G.X.Y., Larkin, K.A., Luca, V.C., Chia, L.A., Mah, A.T., Han, A., Terry, J.M., et al. (2017). Non-equivalence of Wnt and R-spondin ligands during Lgr5+ intestinal stem-cell self-renewal. Nature *545*, 238–242.

Yusa, K., Zhou, L., Li, M.A., Bradley, A., and Craig, N.L. (2011). A hyperactive piggyBac transposase for mammalian applications. Proc. Natl. Acad. Sci. USA *108*, 1531–1536.

Yuzugullu, H., Benhaj, K., Ozturk, N., Senturk, S., Celik, E., Toylu, A., Tasdemir, N., Yilmaz, M., Erdal, E., Akcali, K.C., et al. (2009). Canonical Wnt signaling is antagonized by noncanonical Wnt5a in hepatocellular carcinoma cells. Mol. Cancer *8*, 90.

Zeilstra, J., Joosten, S.P., van Andel, H., Tolg, C., Berns, A., Snoek, M., van de Wetering, M., Spaargaren, M., Clevers, H., and Pals, S.T. (2014). Stem cell CD44v isoforms promote intestinal cancer formation in Apc(min) mice downstream of Wnt signaling. Oncogene *33*, 665–670.

Zhao, C., Sun, G., Li, S., Lang, M.F., Yang, S., Li, W., and Shi, Y. (2010). MicroRNA let-7b regulates neural stem cell proliferation and differentiation by targeting nuclear receptor TLX signaling. Proc. Natl. Acad. Sci. USA *107*, 1876–1881.

Zheng, H., Ying, H., Wiedemeyer, R., Yan, H., Quayle, S.N., Ivanova, E.V., Paik, J.H., Zhang, H., Xiao, Y., Perry, S.R., et al. (2010). PLAGL2 regulates Wnt signaling to impede differentiation in neural stem cells and gliomas. Cancer Cell *17*, 497–509.

Stem Cell Reports, Volume *11*

Supplemental Information

The Zinc Finger Transcription Factor PLAGL2 Enhances Stem Cell Fate and Activates Expression of *ASCL2* in Intestinal Epithelial Cells

Ashlee M. Strubberg, Daniel A. Veronese Paniagua, Tingting Zhao, Leeran Dublin, Thomas Pritchard, Peter O. Bayguinov, James A.J. Fitzpatrick, and Blair B. Madison

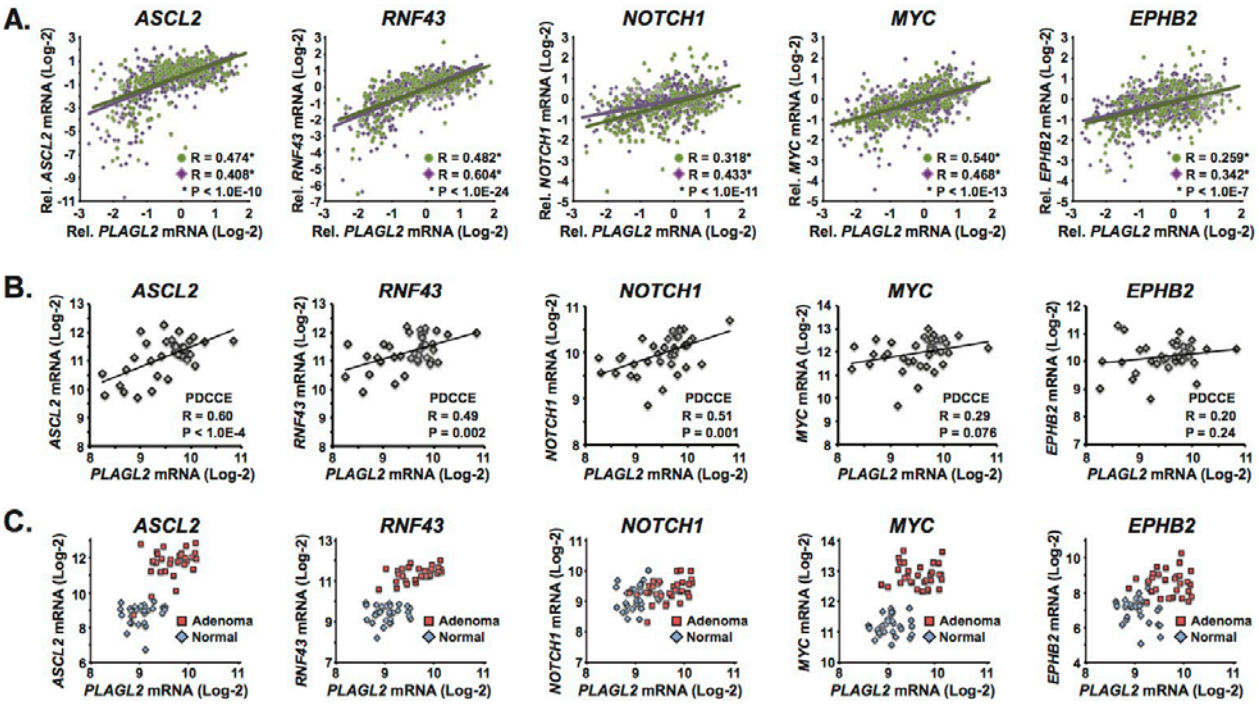

Figure S1. PLAGL2 Expression Correlates with Multiple Stem Cell Markers in Colorectal Cancers and Adenomas. Related to Figure 5. A) Scatter plots of *PLAGL2* mRNA expression vs. stem cell markers as determined from RNA-seq data of CRC tumors from TCGA (Cancer Genome Atlas 2012). Regression analysis indicates a significant positive correlation between these markers and *PLAGL2.* **B)** Scatter plots of *PLAGL2* mRNA expression vs. stem cell markers as determined from Affymetrix microarray analysis of a panel of 27 patient-derived colorectal cancer explants (PDCCEs) performed by Uronis et al. (Uronis et al. 2012). Regression analysis indicates a significant positive correlation between *ASCL2*, *RNF43*, *NOTCH1,* and *PLAGL2.* **C)** Scatter plots of *PLAGL2* mRNA expression vs. stem cell markers as determined from Affymetrix microarray analysis of 32 colorectal adenomas along with matched normal tissue from the same patients performed by Sabates-Bellver et al. (Sabates-Bellver et al. 2007).

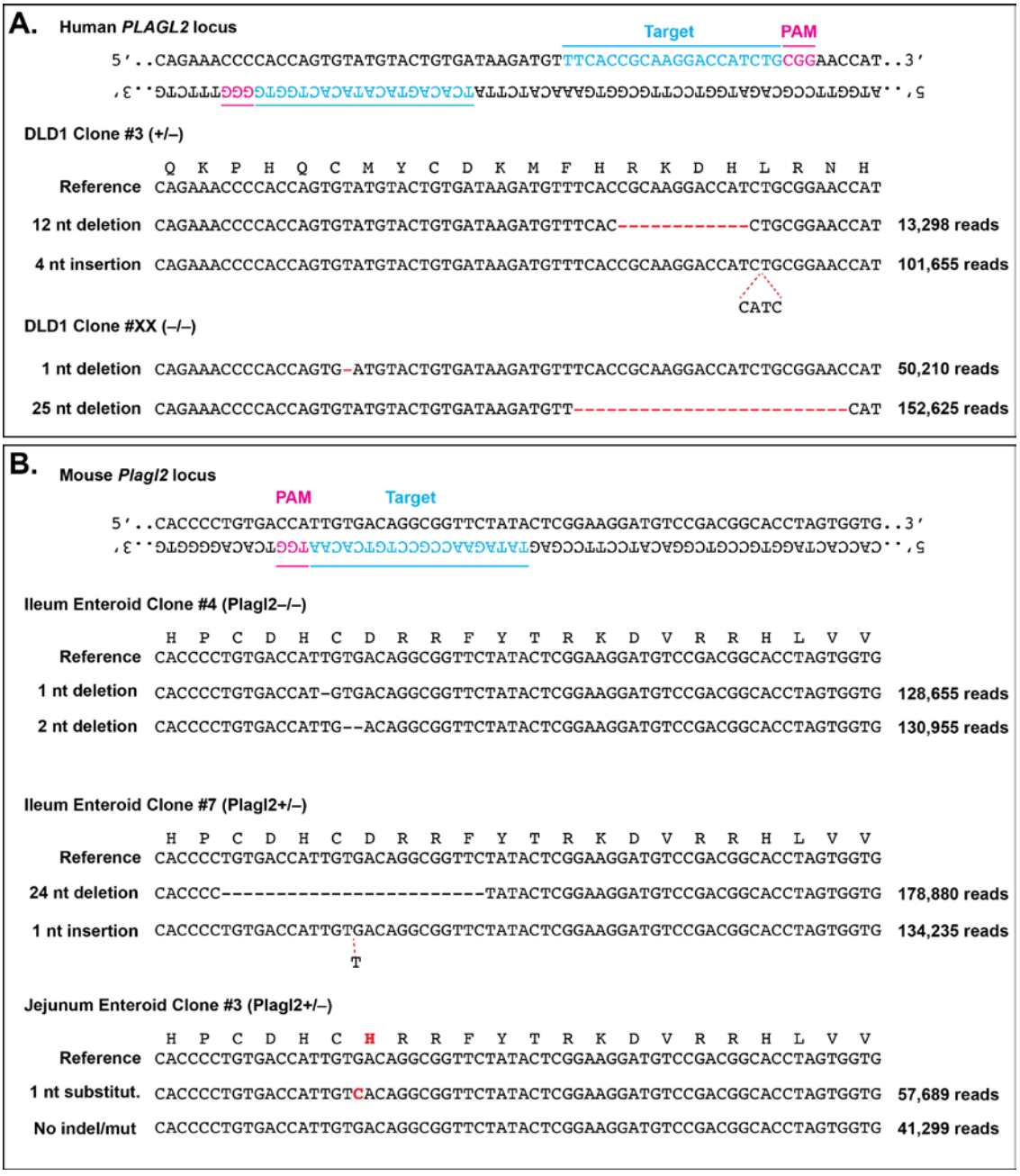

Figure S2. Mutagenesis of *PLAGL2* in DLD1 CRC Cells. Related to Figure 2, 3, and 5. A) The human *PLAGL2* gene was targeted using the CRISPR/Cas paired nickase in conjunction with SRIRACCHA enrichment using the *Piggybac* DNA transposon (Wen et al. 2017). **Top)** Schematic of target site within the *PLAGL2* gene with each CRISPR/Cas paired nickase half site indicated in blue and PAM depicted in pink. **Middle)** Illumina deep sequencing of DLD1 mutant clone #3, which revealed two mutations, one with an in-frame 12 nt deletion, and another mutation with an out-of-frame insertion of 4 nt. **Bottom)** Illumina deep sequencing of DLD1 mutant clone #XX, which revealed two mutations, one with an out-of-frame deletion of 1 nt, and another mutation with an out-of-frame deletion of 25 nt. **B)** The mouse *Plagl2* gene was targeted using CRISPR/Cas in C57BL/6 ileum and jejunum enteroids. **Top)** Schematic of target site within the *Plagl2* gene with the CRISPR/Cas site indicated in blue and PAM depicted in pink. Three mutants were identified and used for experiments. Mutations identified from Illumina sequencing are indicated for clones #4, 7, and 3. Clone #4 possessed two frame-shift mutations. Clone #7 possessed two mutations, one of which generated a frame-shift. Lastly, clone #3 possessed a D197H missense mutation.

Table S1. Oligos and PCR primers used for Cloning. Related to Experimental Procedures.

Primer/Oligo Name	Sequence	Purpose
hPLAGL2_1221(F)	ATCCTCACCTATCTCTTCCCC	Cloning human *PLAGL2* 3'UTR
hPLAGL2_5777(R)	TTTTACTGTCTGCCCTACGC	
SacII_PLAGL23pUTR(F)	TCTCTTCCGCGGCTCAGCTCCCTCCAAAAT	Cloning human *PLAGL2* 3'UTR
MluI_PLAGL23pUTR(R)	TGCCCTACGCGTACCATCATCCTGGATGC TAAAG	
PLAGL2_Let7s1_Kpn(S)	CTCCAAAATACCAGCTTGGATCGGTACC ATACTTGCCCGACAAATTGCCC	Site directed mutagenesis of Let-7 site #1
PLAGL2_Let7s1_Kpn(AS)	GGGCAATTTGTCGGGCAAGTATGGTACC GATCCAAGCTGGTATTTTGGAG	
PLAGL2_Let7s2_Kpn(S)	CTCTGATTCAGAAACACACTTCGGTACCT TTACTGTTAACTCTTAACAGA	Site directed mutagenesis of Let-7 site #2
PLAGL2_Let7s2_Kpn(AS)	TCTGTTAAGAGTTAACAGTAAAGGTACC GAAGTGTGTTTCTGAATCAGAG	
SfiI_Ascl2-1191(F)	CTAAAGGGCCTCCATGGCCTGGAAGTTT GAAGG	Cloning mouse *Ascl2* proximal promoter.
SfiI_Ascl2+312(R)	GTTCATGGCCTAGTGGGCCTGCTTCCATG CTCCGGGC	
PLAGL2_TS_T1(F2)	TGACTGGAGTTCAGACGTGTGCTCTTCCG ATCTATCTCCCCTCTTTCTGCTTTC	For PCR of *PLAGL2* mutations and Illumina Sequencing
PLAGL2_TS_T1(R2)	ACACTCTTTCCCTACACGACGCTCTTCCG ATCTTTGTTAGGATCATGGGTCTGC	
PLAGL2_BsmBI(F)	TGCCATCGTCTCAGGCATGACCACATTTT TCACCAGC	For PCR amp of hPLAGL2 for cloning into expression vectors.
PLAGL2_BsmBI(R)	AGGCTCCGTCTCGTAGCCAAAAACTGAG CTGAGG	
XbaI-hLIN28B(F)	GCCTACTCTAGAGCCACCATGGCCGAAG GC	For PCR amp of hLIN28B for cloning into expression vectors.
EcoRV-hLIN28B(R)	GGCCGCGATATCCGATTTGGCTAGCTTAT GTCTTTTTCC	
hASCL2_BbsI(F)	CTCTAGGAAGACCCGGCATGGACGGCGG CACAC	For PCR amp of hASCL2 for cloning into expression vectors.
hASCL2_BbsI(R)	ATTCGAGAAGACCATAGCTCGAGGGCGC TCAGTAG	
BsaI_GGCA_NLS_Cas9(F)	CGATGTGGTCTCCGGCATGTCGCCGAAG AAAAAGCGCAAG	For PCR amp of Cas9^{D10A} for cloning into expression vectors.
BsaI_ACTC_Cas9(R)	TCATGTGGTCTCCACTCGTATCGATAATT CTTAGCTGGCCTC	
mPlagl2_T5PSL(S)	CACCGTATAGAACCGCCTGTCACAA	For cloning *Plagl2*-specific gRNAs into pBS-U6gRNA
mPlagl2_T5PSL(AS)	AAACTTGTGACAGGCGGTTCTATAC	
mPlagl2_T5PSR(S)	CACCGGATGTCCGACGGCACCTAG	For cloning *Plagl2*-specific gRNAs into pBS-U6gRNA
mPlagl2_T5PSR(AS)	AAACCTAGGTGCCGTCGGACATCC	
LacZOm_T3PSL(S)	CACCGAAGGCGGCGGGCCATTACC	For cloning *LacZ*-specific gRNAs into pBS-U6gRNA
LacZOm_T3PSL(AS)	AAACGGTAATGGCCCGCCGCCTTC	
LacZOm_T3PSR(S)	ACACCGCGTTCGACCCAGGCGTTAG	For cloning *LacZ*-specific gRNAs into pBS-U6gRNA
LacZOm_T3PSR(AS)	AAAACTAACGCCTGGGTCGAACGCG	
BglI_U6gRNA(F)	GGAAAAGGCCTCCAGGGCCGCCCCCTTC ACCGAGGGCCTATTTCCC	For PCR of U6gRNAs from pBS-U6gRNA for cloning into BII-gR-PGW.
BglI_U6gRNA(R)	CTGCAGGCCTTGGAGGCAAAAACAAAAA AGCACCGAC	

Table S2. RT-PCR primers. Related to Experimental Procedures.

Primer/Oligo Name	Sequence	Purpose
PLAGL2(F)	CAGAGACCATATAGCTGCCC	RT-PCR for *PLAGL2*
PLAGL2(R)	CCTTGCGGTGAAACATCTTATC	
ASCL2(F)	CGTTCCGCCTACTCGTC	RT-PCR for *ASCL2*
ASCL2(R)	TGAGGCTCATAGGTCGAGG	
HMGA2(F)	CTATCACCTCATCTCCCGAAAG	RT-PCR for *HMGA2*
HMGA2(R)	GTTGTCCCTGGGCTGAAG	
B2M(F)	TCGCGCTACTCTCTCTTTCT	RT-PCR for *B2M*
B2M(R)	TTTCCATTCTCTGCTGGATGAC	
PPIA(F)	TGCAGACAAGGTCCCAAAG	RT-PCR for *PPIA*
PPIA(R)	CCTGACACATAAACCCTGGAATA	
mWnt9b(F)	GTGTGGTGACAATCTGAAG	RT-PCR for mouse *Wnt9b*
mWnt9b(R)	TCCAACAGGTACGAACAG	
mWnt4(F)	AGTGCCAATACCAGTTCCG	RT-PCR for mouse *Wnt4*
mWnt4(R)	AGAGATGGCGTATACAAAGGC	
mWnt10a(F)	CGCTTCTCTAAGGACTTTCTGG	RT-PCR for mouse *Wnt10a*
mWnt10a(R)	GTGGCATTTGCACTTACGC	
mWnt5a(F)	CGCTAGAGAAAGGGAACGAATC	RT-PCR for mouse *Wnt5a*
mWnt5a(R)	CTCCATGACACTTACAGGCTAC	
Ascl2(F)	GGCTGCTCTGAGCCTACCT	RT-PCR for mouse *Ascl2*
Ascl2(R)	TAGGTCCACCAGGAGTCACC	
Axin2(F)	TAGGTTCCGGCTATGTCTTTG	RT-PCR for mouse *Axin2*
Axin2(R)	TGTTTCTTACTCCCCATGCG	
Cd44(F)	TTCATCCCAACGCTATCTGTG	RT-PCR for mouse *Cd44*
Cd44(R)	CGAAGGAATTGGGTAGGTCTG	
Wintrlinc1(F)	TTGCTGAAAGGACTGGTCTG	RT-PCR for mouse *Wintrlinc1*
Wintrlinc1(R)	GGATGTGGGTGAAGTGGAC	
Hprt(F)	CCCCAAAATGGTTAAGGTTGC	RT-PCR for mouse *Hprt*
Hprt(R)	AACAAAGTCTGGCCTGTATCC	
Tbp(F)	CACCAATGACTCCTATGACCC	RT-PCR for mouse *Tbp*
Tbp(R)	CAAGTTTACAGCCAAGATTCACG	

Table S3. Oligos used for gRNA Cloning/Generation. Related to Experimental Procedures.

Primer/Oligo Name	Sequence	Purpose
PLAGL2_T1PSR(S)	CACCGTTCACCGCAAGGACCATCTG	PLAGL2 gRNA T1 oligos for cloning into pBS-U6gRNAx2
PLAGL2_T1PSR(AS)	AAACCAGATGGTCCTTGCGGTGAAC	
PLAGL2_T1PSL(S)	ACACCGTCACAGTACATACACTGGTGG	PLAGL2 gRNA T1 oligos for cloning into pBS-U6gRNAx2
PLAGL2_T1PSL(AS)	AAAACCACCAGTGTATGTACTGTGACG	
PLAGL2_T2PSR(S)	CACCGATCTCATACCGTAGGACTTC	PLAGL2 gRNA T2 oligos for cloning into pBS-U6gRNAx2
PLAGL2_T2PSR(AS)	AAACGAAGTCCTACGGTATGAGATC	
PLAGL2_T2PSL(S)	ACACCGTTTCACGGGGTTGGGGCTCAG	PLAGL2 gRNA T2 oligos for cloning into pBS-U6gRNAx2
PLAGL2_T2PSL(AS)	AAAACTGAGCCCCAACCCCGTGAAACG	
PLAGL2_T1(S)	GTGACCCCACCAGTGTATGTACTGTGATAAGATGTTTCACCGCAAGGACCATCTGCG	CRISPR/Cas9 target site 1 oligos for cloning into BII-C3HTK
PLAGL2_T1(AS)	GTCACCGCAGATGGTCCTTGCGGTGAAACATCTTATCACAGTACATACACTGGTGGG	
PLAGL2_T2(S)	GTGACCTTGAGCCCCAACCCCGTGAAAAGATCTCATACCGTAGGACTTCAG	CRISPR/Cas9 target site 2 oligos for cloning into BII-C3H2B
PLAGL2_T2(AS)	GTCACCTGAAGTCCTACGGTATGAGATCTTTTCACGGGGTTGGGGCTCAAG	

SUPPLEMENTAL EXPERIMENTAL PROCEDURES

Vector Construction

The BII-ChBt and BII-ChPt *Piggybac* transposon vectors consist of the CpG-less human EF1alpha promoter downstream of the CMV enhancer (ChEf1a promoter, Invivogen Inc.) a Blasticidin (ChBt) or Puromycin (ChPt) resistance cassette, the T2A peptide, a Flag (ChBt) or HA (ChPt) epitope tag, and a cloning site (AGCGGCAT**GAGACG**GATAGCT**CGTCTC**AGCTA) for cDNA expression.

Fluorescent Reporter for Assaying miRNA Effects on the *PLAGL2* 3' UTR

A Piggybac DNA transposon vector (BII-BCnDFP) was generated, consisting of CMV-driven expression of puromycin N-acetyltransferase fused via a T2A self-cleaving peptide to a destabilized nuclear-targeted tandem Tomato (DD-tdT-NLS) red fluorescent protein. The destabilization domain (DD) is a 107-amino acid sequence from the FKBP1A protein possessing the L106P and F36V mutations (Egeler, Urner et al. 2011). Downstream of DD-tdT-NLS is the miRNA, such as Let-7a, for constitutive expression. The Let-7a chimeric shRNA (Let7a155) contains a modified terminal loop from mir155, as previously described (Madison, Liu et al. 2013), and was cloned from a BamHI and XhoI fragment from the pcDNA6.2-Let-7a vector and inserted upstream of the SV40 late polyadenylation signal. As a negative control, a non-specific shRNA was similarly cloned from the pcDNA6.2-GW/EmGFP-miR vector (Thermo Fisher Scientific). Downstream of this is a CMV-driven destabilized EGFP (dGFP) protein with a 40-amino acid PEST destabilization domain (from the mouse ODC protein) fused to the EGFP C-terminus, as previously characterized (Li, Zhao et al. 1998). Downstream of this is a multiple cloning site (MCS) containing restriction sites for SacII, ApaI, MluI, KpnI, and XbaI, followed by two copies of the 240 bp chicken beta globin hypersensitive site IV core insulator element (Chung, Bell et al. 1997). To construct a Let-7 sensitive synthetic reporter with Let-7 recognition sequences, a Let-7 sponge sequence and bovine growth hormone polyadenylation signal (BGHpA) were PCR amplified from the pRNA-U6-let7 sponge (gift from Phillip Zamore, Addgene plasmid # 35664) and cloned into the XbaI site in BII-BCnDFP.

Assaying Ascl2 Promoter Activity with a Fluorescent Reporter

To construct the BII-BCA vector for assaying Ascl2 promoter activity, the 5' CMV promoter was removed and replaced with one copy of the 240 bp chicken beta globin hypersensitive site IV core insulator element (Chung, Bell et al. 1997), followed by the human adenovirus type 2 splice acceptor and the polyadenylation signal from the HSV thymidine kinase gene, and two copies of a directional polylinker consisting of two SfiI sites. The 3' CMV was replaced with the CpG-less human EF1alpha promoter downstream of the CMV enhancer (ChEf1a promoter, Invivogen Inc.).

Human and Murine Organoid Culture Medium

Human organoids were maintained in basal medium (Advanced DMEM/F12, 1x Penicillin/Streptomycin, 1x Glutamax, 1x HEPES) containing R-spondin-1 (10%), Noggin (10%), Wnt3a (25%), 50ng/mL EGF (Cat # 236-EG, R&D Systems), 0.5µM A83-01 (Tocris), 10nM Gastrin (Millipore-Sigma), 1mM N-Acetylcysteine (Millipore-Sigma), 3µM SB202190, and 1x B27 (collectively termed WENRAS). For colony formation assays, human organoids were cultured for 4-5 days prior in basal medium containing R-spondin-1 (10%), Noggin (10%), 50ng/mL EGF (Cat # 236-EG, R&D Systems), 0.5µM A83-01 (Tocris), 10nM Gastrin (Millipore-Sigma), 1mM N-Acetylcysteine (Millipore-Sigma), and 1x B27 (termed differentiation medium, ENRA). Noggin, R-spondin1, and Wnt3a conditioned media were produced as previously described (Wen, Liao et al. 2017).

Murine enteroids were established from cultured crypts freshly isolated from 6-8 week old C57BL/6 mice, which were maintained on a 12 hour light/dark cycle and provided with food (standard mouse chow) and water, *ad libitum*. Enteroids maintained in ENR medium containing R-spondin-1 (10%), Noggin (10%), 50ng/mL EGF (Cat # 236-EG, R&D Systems), 1mM N-Acetylcysteine (Millipore-Sigma), 1x N2, and 1x B27 (Sato, Vries et al. 2009). Prior to transfection, murine enteroids were expanded for 3 days in ENR medium supplemented with 10 mM nicotinamide and 25% Wnt3a conditioned medium (ENRW-Nic).

Human Organoid Transfection

Organoids were cultured 72 hours in medium without Wnt3a containing 4 µM Chir99021 (ENRAS-C), then with 10 µM Y27632 (ENRAS-CY) for 48 hours, and 1.25% dimethylsulfoxide (ENRAS-CYD) 24 hours prior to transfection. Organoids were dissociated for 20 minutes in TrypLE Express (Thermo Fisher Scientific), then spinoculated for 1 hour in 24-well plates at 600 x g, at 26° to 32°C, with 1 µg DNA (200 ng pCMV-hyPBase, 800

ng BII-ChPt-PLAGL2 or PB533A-LIN28B) and 3 µl Lipofectamine 2000 in 500 µl ENRAS-CYD. After 10 days in culture, Puromycin/G418 resistant colonies were individually expanded and expression verified by RT-PCR.

Colony Forming Assays

For human organoid colony forming assays, organoids were dissociated in TrypLE Express (Life Technologies) containing 250 U/mL DNase I (1:200, NEB) and 10 µM Y27632 (Selleck Chemicals) for 20 minutes at 37ºC. Cells were then incubated at room temperature in basal medium (Advanced DMEM/F12, 1x Penicillin/Streptomycin, 1x Glutamax, 1x HEPES) containing DNase I and Y27632 for 5 mins with periodic vortexing. Single cells were plated in quadruplicate at 5,000 cells/well on a 24-well plate (Greiner) in 80% Matrigel, 20% ENR with 10 µM Y27632, and overlaid with WENRAS plus 10 µM Y27632. Y27632 was removed on day 4 post- plating. Images were taken and quantified at day 0 and day 7 (LIN28B organoids) or day 10 (PLAGL2 organoids) post-plating using a Biotek Cytation3 Imaging Platform with Gen5 software.

For mouse enteroid colony forming assays, enteroids were dissociated in TrypLE Express containing 250 U/mL DNase I and 10 µM Y27632 for 5 minutes at 37ºC. Cells were then incubated at room temperature in ENR containing DNase I and Y27632 for 5 mins with periodic vortexing. Single cells were plated in quadruplicate at 5,000 cells/well on a 24-well plate in 80% Matrigel, 20% ENR with 10 µM Y27632, and overlaid with ENR plus 10 µM Y27632. Y27632 was removed on day 4 days post-plating. Cultures were imaged and quantified on days 0 and 7 post-plating using a Biotek Cytation3 Imaging Platform with Gen5 software.

Preparation of Sections for EdU Staining

To de-paraffinize, sections were washed for 5 minutes each in Histoclear 3x, 100% ethanol 2x, 90% ethanol 1x, 70% ethanol 1x, 50% ethanol 1x, dH_2O 1x, and 1x PBS 3x. Antigen retrieval was performed by incubating sections in sodium citrate buffer (10 mM sodium citrate, 0.05% Tween 20, pH 6.0) in a pressure cooker for 5 minutes at high pressure, cooled to room temperature, then rinsed 3x in 1x PBS.

Mutagenesis of Plagl2 in Mouse Enteroids

For generating knock-outs of mouse *Plagl2* C57BL/6 jejunum and ileum enteroids (from 6-8 week old mice, each at passage #1) were expanded for transfection as described above. Enteroids were transfected with 500 ng hCas9 (Addgene Plasmid # 41815), 300 ng of BII-ChPtG (encoding GFP), 100 ng of pBS-U6-gRNA (Wen, Liao et al. 2017), and 100 ng of pCMV-hyPBase. Selection with Puromycin (Invivogen, 2 µg/ml) was initiated 72 hours after transfection. After 7 days Puromycin selection, individual colonies were picked, and expanded for genotyping by Illumina sequencing. Genomic DNA (gDNA) was extracted and the targeted region of *Plagl2* was amplified by PCR with Q5 DNA polymerase for amplicon Illumina sequencing through the Washington University Center for Genomic Sciences. Sequence was analyzed using CRISPresso (Pinello, Canver et al. 2016) to characterize any mutant alleles. Two mutant ileum enteroid clones were identified, one (#4) with no WT allele detected, but only two frame-shift alleles, while the other clone (#7) also had no detectable WT allele but possessed only one out-of-frame allele, and is suspected to be a functional heterozygote. One mutant jejunum clone (#3) had one missense mutation and is also a suspected functional heterozygote, but because this jejunum *Plagl2* mutant allele may not represent a loss of function mutation, most experiments were performed on the ileum enteroid *Plagl2* mutants. Enteroid growth of mutants was quantified using the Biotek Cytation3 and colony forming assays were performed as above. Enteroid clones targeted with *Plagl2* gRNAs, which exhibited no mutations by Illumina sequencing, were used as WT controls. For RT-PCR RNA was extracted from WT control and *Plagl2* mutant enteroids using Trizol (Thermo Fisher Scientific). RT reactions were performed on 1-3 µg total RNA with Superscript III (Thermo Fisher Scientific) and oligo dT primers, followed by QPCR with Bullseye Evagreen 2x QPCR Mix (MidSci).

Transient Mutagenesis of *Plagl2* and Lineage Tracing in Mouse Enteroids

Enteroids constitutively expressing $Cas9^{D10A}$ were first generated by integrating a stable *Piggybac* transgene, BII-ChPt-$Cas9^{D10A}$, into C57BL/6 jejunum enteroids (from 6-8 week old mice, at passage #4). The $Cas9^{D10A}$ nickase variant was implemented here to minimize the chances of off-target gRNA-independent mutations that might be caused by constitutive long-term nuclease expression in enteroids (Ran, Hsu et al. 2013). All Puromycin-surviving clones (n = 12) were pooled and expanded for subsequent transfection with a gRNA-expressing transposon. Expression of the HA-tagged $Cas9^{D10A}$ nickase in these enteroids was confirmed by immunoblot (data not shown) as described above. The BII-ChPtG vector was modified for gRNA expression by cloning a PCR fragment for two U6-gRNA expression cassettes from the pBS-U6-gRNA vector, containing gRNAs against the *Plagl2* gene or bacterial beta-galactosidase, LacZ (NS control). The two cassettes were ligated together through unique BsaI sites, cut with BglI, and then cloned into a unique SfiI site located within the BII-ChPtG vector,

just upstream of the ChEf1a promoter. This generated the BII-gRx2-PtG vector. For lineage tracing experiments, $Cas9^{D10A}$ enteroids were transfected with 200 ng pCMV-hyPBase and 800 ng of a BII-gRx2-PtG vector targeting the *Plagl2* gene or LacZ (NS control). After transfection, enteroids were plated in a 6-well plate, in triplicate, and were imaged daily using the Biotek Cytation3 for EGFP fluorescence and brightfield images beginning 4 days after transfection. At 7 days after transfection, the number of GFP-positive lineage tracing events was quantified by counting the number of GFP-positive clones having a size greater than >150 μm in diameter, and qualitatively comprising a whole organoid, or a part of an organoid, including at least one or two whole buds. For simultaneous over-expression of ASCL2 for rescue, enteroids (passage #) were transfected as above with 200 ng pCMV-hyPBase, 400 ng of a BII-gRx2-PtG vector, and 400 ng of a BII-ChBt-ASCL2/BII-ChBt (empty). Enteroids were plated in a 6-well plate, as above, in triplicate and selection with 5 μg/ml Blasticidin was initiated at 72 hours and the numbers of initial live enteroids were quantified using the Cytation3. Enteroids were imaged every 48 hours for 7 days, and GFP-positive clones were quantified as above on day 7. Percentages of GFP-positive clones were expressed relative to the numbers of initially live enteroids, prior to Blasticidin. Blasticidin resistant colonies were pooled and genotyped as above by Illumina sequencing and analyzed using CRISPResso (Pinello, Canver et al. 2016)). Mutant alleles were quantified as present if such mutations yielded 10 or more reads per mutation. Genomic DNA was also analyzed for indels at *Plagl2* by T7E1 assay, as previously described (Wen, Liao et al. 2017).

Wnt Reporter (TOP-tdT) Construction and Transfection

The promoter and TCF/Lef sites from the M50 Super 8x TOPFlash vector (a gift from Randall Moon, Addgene plasmid # 12456, (Veeman, Slusarski et al. 2003)) was PCR amplified with Q5 polymerase (NEB) with primers containing BglI sites, and cloned into the unique SfiI sites of the BII-BCA vector, to create the BII-BCA-TOPFlash vector. The destabilization domain of tdTomato and the EGFP expression cassette were then each deleted by site-directed mutagenesis to create the BII-TOP-tdT vector.

Transection of mouse ileum or jejunum enteroids with pCMV-hyPBase (200 ng), BII-TOP-tdT (400 ng), and BII-ChPt-PLAGL2 (400 ng) was performed at passage 4. Negative controls were either empty vector (BII-ChPt) or BII-ChPt-EGFP. After 7 days selection with Puromycin (Invivogen, 2 μg/ml), individual RFP-positive colonies were picked, expanded, and verified for expression of human PLAGL2 by RT-PCR. Fluorescence in enteroids was measured in organoids by three methods: **1)** enteroid colonies were imaged using the Cytation3, and total and mean tdTomato fluorescence was calculated for each enteroid using Gen5 software, **2)** enteroids were dissociated 5 minutes with TrypLE (Thermo Fisher Scientific) containing 10 μM Y27632, neutralized with an equal volume of ENR medium containing 10 μM Y27632, centrifuged 45 seconds at 1500 x g, and re-suspended in 15 μl complete ENR medium containing 10 μM Y27632, cover-slipped onto Superfrost Plus (Thermo Fisher Scientific) microscope slides, and tdTomato fluorescence measured by imaging single cells with the Cytation3, **3)** live enteroids in 35 mm tissue culture dishes were passaged and imaged at 72 hours after a 1 hour incubation with 5 μg/ml Hoechst 33342 (Thermo Fisher Scientific). Organoid cultures were visualized using an upright Zeiss Examiner.Z1-based 880 LSM with a 20x/1.0 water-immersion objective. Hoechst dye was excited using a 405 nm diode laser and tdTomato was excited with a 561 nm DPSS laser. Optical sections (0.5 μm) were acquired with an Airyscan super-resolution detector and were processed using ZEN Blue v. 2.3.

Enteroid Co-Culture

For examining effects on Wnt signaling through secreted factors, control EGFP-expressing enteroids possessing the TOP-tdT reporter were cultured in ENR medium in a 50/50 mixture with PLAGL2-expressing enteroids or alone, in 24-well plates (Greiner), in quadruplicate. Cultures were then imaged at days 0, 2, 6, 8, and 10 for EGFP and tdTomato fluorescence. For co-culture and colony forming assays, PLAGL2-expressing enteroids (clone #1 and #2) were incubated in a 50/50 mix with WT jejunum enteroids established from $R26^{mTmG}$ mice (passage #3), which constitutively express membrane-localized tdTomato. After 72 hours of co-culture, enteroids were dissociated and 10,000 cells were plated per well in a 24-well plate, in quadruplicate. At d0, just after plating in matrigel, tdTomato positive $R26^{mTmG}$ cells were counted with the Cytation3 to quantify the number of WT/control cells. At d7, tdTomato positive enteroid colonies were counted with the Cytation3.

Inhibiting Wnt Signaling in TOP-tdT/PLAGL2 O/E Enteroids

Ileum enteroids transfected with BII-ChPt-PLAGL2 or BII-ChPtG-EGFP and the TOP-tdT reporter were plated in 24 well plates and treated with 2 μM IWP-2 or vehicle (0.1% DMSO), in triplicate. Fluorescent and bright-field images were taken every 24 hours with the Cytation3, and medium was changed, with fresh IWP-2/DMSO, every 48 hours. In separate experiments enteroids were collected at 48 hours for RNA extraction (Trizol, Thermo Fisher Scientific) and RT-PCR for *Ascl2, Lgr5, Cd44, Axin2,* and *Ets2.* For examining effects on enteroid survival,

IWP-2 treatment was continued for a total of 6 days, 48 hours after the complete disappearance of TOP-tdT fluorescence. Remaining dead/dying enteroids were then mechanically dissociated and re-plated in 12-well plates and fresh ENR medium added to gauge enteroid recovery. After 2 weeks of recovery in ENR, enteroids were imaged with the Cytation3 and colonies counted using Gen5 software.

Western Blots (IB)

To quantify protein levels by IB, enteroid lysates were prepared using 1x Cell Lysis Buffer (#9803, CST) supplemented with 1x protease inhibitor cocktail (P8340, Sigma), 2 mM Na_3VO_4, and 5 mM sodium pyrophosphate. Lysates were run on Biorad pre-cast acrylamide gels and transferred to nylon membranes using the Trans-Blot Turbo System (Bio-Rad). After blocking with 5% BSA in Tris-buffered saline and 0.1% Tween-20, IB was performed using rabbit anti-HA (#3724, CST) or mouse anti-Tubulin (sc-8035, CST) at a 1:1000 dilution and visualized with near-infrared fluorescent conjugated secondary antibodies (1:10,000 dilution) on an Odyssey CLx near-infrared fluorescence imaging system (LiCor).

Fluorescent Reporter for Assaying miRNA Effects on the *PLAGL2* 3'UTR

To assay sensitivity of the Let-7 reporter to Let-7, $1x10^5$ DLD1 cells were seeded on 24-well plates in quadruplicate and transfected the next day with 400 ng of the BII-BCnDFP vector with the Let-7 sponge (BII-BCnDFP-L7spo) and 100 ng of pCMV-hyPBase. The miRNA cloned into this vector was either a non-specific or Let-7a chimeric shRNA. After 48 hours, Puromycin (5 µg/ml) was added and fluorescence was measured every 24-48 hours using a Biotek Cytation3 with Gen5 software.

To assay sensitivity of the PLAGL2 3'UTR, this sequence was PCR amplified from normal human genomic DNA (gDNA) (primers in Table S1) and sub-cloned into the SacII and MluI restriction sites in the BII-BCnDFP vector, just 3' of the dGFP sequence. Mutations in the Let-7 sequences in the PLAGL2 3'UTR was performed by site-directed mutagenesis using Q5 DNA polymerase (NEB). Adaptation for use with the Q5 polymerase entailed dilution of mutagenesis reactions 1:4 with 1x Cutsmart buffer (NEB) prior to a 1 hour digestion with 20 units of DpnI. To assay sensitivity of the PLAGL2 3'UTR to Let-7, transfections were performed as above, and fluorescence measured after 7 days of Puromycin (5 µg/ml) selection.

Assaying Ascl2 Promoter Activity with a Fluorescent Reporter

The proximal 1.47 Kb region of the mouse *Ascl2* promoter was cloned into the BII-BCA vector at SfiI sites (primers listed in Table S1). To test reporter response to PLAGL2 over-expression, 100 ng of pCMV-hyPBase and 300 ng of the BII-BCA-Ascl2 vector was co-transfected with 100 ng of BII-ChBt (empty) or BII-ChBt-PLAGL2 vector in DLD1 cells using 1 µl of JetPrime Transfection Reagent according to manufacturer's instructions. After 48 hours, cells were selected for 5 days with 10 µg/ml Blasticidin (MilliporeSigma), and fluorescence measured on day 6. To test reporter response to *PLAGL2* knock-down, DLD1 cells were transfected in 6-well plates with 400 ng of pCMV-hyPBase, 1400 ng of the BII-BCA-Ascl2 vector, and 200 ng of BII-ChPt empty vector. 48 hours later, cells were selected with 5 µg/ml Puromycin for 3 days, then expanded without Puromycin for 3 additional days. Cells were then plated in 24-well plates for transfection with 5 pmoles *PLAGL2* siRNAs (IDT, Inc.) and 1.5 µl Lipofectamine RNAiMAX (ThermoFisher). Fluorescence was read 72 hours later on a Biotek Cytation3 Imaging Platform with Gen5 software.

EdU Incorporation Assays in Human Colonoids

To measure proliferation, organoid cultures were exposed to 10 µM EdU for 1 hour and fixed at room temperature in 4% paraformaldehyde (PFA) for 90 minutes. Organoids were then suspended in a pre-warmed 2% agar solution (MilliporeSigma), transferred to molds, and incubated in a 50°C oven for 5 minutes to allow organoid settling for optimal sectioning. Molds were transferred to 4°C for solidification, then embedded in paraffin and sectioned onto microscope slides by the Digestive Diseases Research Core Center (DDRCC) at Washington University in St. Louis. The Click-iT™ Plus EdU Alexa Fluor 488 Imaging Kit (Thermo Fisher) was used to visualize EdU-positive cells per the manufacturer's protocol. Nuclei were stained with Hoechst dye (1:2000) for 1 hour. ProLong™ Diamond Antifade Mountant (Thermo Fisher) and glass coverslip (Fisher Scientific) were added to each slide, then cured 24 hours at room temperature. Images were acquired using a Zeiss Axiovert 200 microscope and Axiocam MRM camera with an Apotome optical sectioning filter (Carl Zeiss, Jena, Germany). To quantify proliferation, the number of EdU-postive and total nuclei were counted as TIFF files in 10-12 frames per clone using ImageJ Software.

Mutagenesis of the *PLAGL2* gene in DLD1 cells

For mutagenesis using SRIRACCHA (Wen et al., 2016), 5 x 10^5 DLD1 cells were plated into one well of a 6-well plate and transfected the next day with 500 ng pCMV-hyPBase, 1 µg of BII-C3HTK-PLAGL2-T1, and 1 µg of BII-C3H2B-PLAGL2-T2 using 5 µl of JetPrime Transfection Reagent. After 48 hours, cells were selected with 5 µg/ml Puromycin for 7 days. Cells were re-plated (5 x 10^5 cells/well) and transfected with 1.2 µg of hCas9-D10A plasmid (a gift from George Church, Addgene plasmid #41816), 250 ng pBS-U6gRNA-PLAGL2-T1, 250 ng pBS-U6gRNA-PLAGL2-T2, 400 ng of pBS-PtH, and 400 ng of pBS-PtH2BG using 5 µl of JetPrime Transfection Reagent. These vector backbones were previously described (Wen et al., 2017). 24 hours later, cells were split between two wells of a 6-well plate, and transfection with CRISPR plasmids was repeated, as above. Cells were then selected 48 hours later with hygromycin (600 µg/ml) for 10 days, and individual GFP-positive hygromycin-resistant colonies were picked, expanded, and gDNA isolated for genotyping.

mRNA-Seq

GFP- and PLAGL2-expressing mouse enteroids were homogenized in Trizol and RNA extracted. Two samples from each line were taken, at passages #3 and #4, for mRNA-seq. Total RNA (5 µg) was incubated with 1 µl (2 U) DNase I and 2 µl of SUPERase-In RNase Inhibitor (Thermo Fisher) in a 50 µl reaction for 10 minutes at 37°C. RNA was purified with the RNeasy Mini RNA Extraction Kit (Qiagen) and eluted with 15 µl nuclease-free ddH_2O. Concentrations were determined with the Qubit RNA BR Assay Kit (Thermo Fisher). Samples were submitted for mRNA-seq to the Washington University GTAC for ribosomal RNA depletion (with Ribo-Zero rRNA Removal Kit, Illumina), sample preparation, and high throughput Illumina deep sequencing. Data analysis by GTAC is provided as follows: reads are trimmed, selected for high-quality (PHRED score > 25), aligned to the genome using bowtie2 (Langmead, Trapnell et al. 2009), and expression based on RPKM (reads per kilobase million) was evaluated by examining differential transcript levels between PLAGL2- and GFP-expressing enteroids. Genes/exons are filtered for just those that are expressed and the results are filtered for just those genes or exons found to be differentially expressed. The number of genes down-regulated or up-regulated >2-fold for each PLAGL2-expressing clone is indicated. GSEA (Figure 3) used a gene set consisting of 600 transcripts up-regulated >3-fold in PLAGL2 #2 enteroids, and up-regulated >1.05-fold in PLAGL2 #1 enteroids, relative to GFP-TG enteroids. The dataset for comparison to this gene set is a ranked list of 3,566 transcripts from Lgr5-EGFP-sorted IESCs selected for up-regulation or down-regulation, relative to Lgr5-$EGFP^{LOW}$ cells ($p<0.05$) from a published dataset (Munoz, Stange et al. 2012)

SUPPLEMENTAL REFERENCES

Chung, J. H., A. C. Bell and G. Felsenfeld (1997). "Characterization of the chicken beta-globin insulator." Proc Natl Acad Sci U S A **94**(2): 575-580.

Egeler, E. L., L. M. Urner, R. Rakhit, C. W. Liu and T. J. Wandless (2011). "Ligand-switchable substrates for a ubiquitin-proteasome system." J Biol Chem **286**(36): 31328-31336.

Langmead, B., C. Trapnell, M. Pop and S. L. Salzberg (2009). "Ultrafast and memory-efficient alignment of short DNA sequences to the human genome." Genome Biol **10**(3): R25.

Li, X., X. Zhao, Y. Fang, X. Jiang, T. Duong, C. Fan, C. C. Huang and S. R. Kain (1998). "Generation of destabilized green fluorescent protein as a transcription reporter." J Biol Chem **273**(52): 34970-34975.

Madison, B. B., Q. Liu, X. Zhong, C. M. Hahn, N. Lin, M. J. Emmett, B. Z. Stanger, J. S. Lee and A. K. Rustgi (2013). "LIN28B promotes growth and tumorigenesis of the intestinal epithelium via Let-7." Genes Dev **27**(20): 2233-2245.

Munoz, J., D. E. Stange, A. G. Schepers, M. van de Wetering, B. K. Koo, S. Itzkovitz, R. Volckmann, K. S. Kung, J. Koster, S. Radulescu, K. Myant, R. Versteeg, O. J. Sansom, J. H. van Es, N. Barker, A. van Oudenaarden, S. Mohammed, A. J. Heck and H. Clevers (2012). "The Lgr5 intestinal stem cell signature: robust expression of proposed quiescent '+4' cell markers." EMBO J **31**(14): 3079-3091.

Pinello, L., M. C. Canver, M. D. Hoban, S. H. Orkin, D. B. Kohn, D. E. Bauer and G. C. Yuan (2016). "Analyzing CRISPR genome-editing experiments with CRISPResso." Nat Biotechnol **34**(7): 695-697.

Ran, F. A., P. D. Hsu, C. Y. Lin, J. S. Gootenberg, S. Konermann, A. E. Trevino, D. A. Scott, A. Inoue, S. Matoba, Y. Zhang and F. Zhang (2013). "Double Nicking by RNA-Guided CRISPR Cas9 for Enhanced Genome Editing Specificity." Cell **154**(6): 1380-1389.

Sato, T., R. G. Vries, H. J. Snippert, M. van de Wetering, N. Barker, D. E. Stange, J. H. van Es, A. Abo, P. Kujala, P. J. Peters and H. Clevers (2009). "Single Lgr5 stem cells build crypt-villus structures in vitro without a mesenchymal niche." Nature **459**(7244): 262-265.

Veeman, M. T., D. C. Slusarski, A. Kaykas, S. H. Louie and R. T. Moon (2003). "Zebrafish prickle, a modulator of noncanonical Wnt/Fz signaling, regulates gastrulation movements." Curr Biol **13**(8): 680-685.
Wen, Y., G. Liao, T. Pritchard, T. T. Zhao, J. P. Connelly, S. M. Pruett-Miller, V. Blanc, N. O. Davidson and B. B. Madison (2017). "A Stable but Reversible Integrated Surrogate Reporter for Assaying CRISPR/Cas9-Stimulated Homology-directed Repair." J Biol Chem.